ADOT PMS Deterioration Curve Development

IMPLEMENTATION REPORT

November 18th, 2024

Contents

Table of Tables

Table of Figures

Version History

Version	Date	Description	Author(s)	Reviewer(s)
1.0	July 16, 2024	Version 1.0	Gabriel Duarte Luna	Jeff Zavitski
1.1	October 25, 2024	Revisions made to the design document following implementation and client comments	Matthew Spataro	Jeff Zavitski
1.11	Nov 18, 2024	Revisions following Maria's comments on Implementation Report	Matthew Spataro	Jeff Zavitski

Document Approval

Name	Title	Signature	Date Signed
Mujeeb Ben-Said	Project Manager		
Jeff Zavitski	Technical Director Asset Management		
Thor Anderson	Performance/ Asset Manager, Multimodal Planning Division		

Glossary

The below table lists acronyms and abbreviation used in this document:

Acronym/Abbreviation	Meaning
ADOT	Arizona Department of Transportation
PMS	Pavement Management System
MAE	Mean Absolute Error
dTIMS	Deighton Total Infrastructure Management System®
BA	Business Analytics®

1 Introduction

The initial version of the ADOT PMS delivered in dTIMS BA by Deighton was finalized in 2020 with the publishing of the final project report. Since that initial implementation, ADOT and Deighton have made minor changes to the PMS configuration focusing on treatments, decision trees, and modifying data loading processes and custom reports as necessary. Since the initial implementation was completed several years ago and the PMS hasn't been updated since, it was a suitable time to update the deterioration models used in the PMS, given the availability of more pavement history data.

This document outlines the implementation of new deterioration curves for the Arizona Department of Transportation (ADOT) Pavement Management System (PMS). Deighton conducted the following:

- Detailed data sources and the methodology used to acquire results.
- Evaluated the accuracy of existing curves using historic data.
- Assessed the statistical significance of pavement families.
- Developed new curves to forecast pavement deterioration using new data.
- Delivered visual representations of data and new curves.
- Analyzed effects of new curve implementation in dTIMS BA.
- Implemented new models in ADOT's BA setup.

This project has resulted in a set of deterioration models that refined the ADOT PMS in dTIMS BA. Deighton believes these models are more accurate than the initial curves developed during the initial implementation. Firstly, there was more deterioration data to pull from. Secondly, Deighton employed new and enhanced data processing methodologies.

This report begins detailing the methodology employed to achieve the results. Section 6 details the results of the deterioration curve development and any other relevant implementation information.

With the implementation of the models in the ADOT on-prem dTIMS BA and with the delivery of this report, the model development project is complete with only on-site training remaining for project wrap up.

2 Data Input and Transformation

Deighton began the project with the Data Input and Transformation phase. In this phase, low quality data was removed, and the data was transformed – enabling comparison with previously generated deterioration curves.

This process started with acquiring existing and newly-sent data from ADOT (Section 2.1) and was followed by its compilation (Section 2.2). Then, to use the data to assess the accuracy of previous deterioration curve families, the data was transformed further.

2.1 Data Input

Deighton used a range of data to achieve the deterioration analysis.

The main data used for this analysis was:

- Condition Data containing yearly condition scores Condition Data (section 2.1.1).
- Inventory Data containing additional information for segments (section 2.1.2).

This section identifies which data was used, the sources of each, their significance, and notes any information regarding the data.

2.1.1 Condition Data

Condition data is the foundation of the deterioration analysis – numerically quantifying how pavements age with time in terms of different condition scores. ADOT provided Deighton with tenth-mile condition data spanning from 2017 to 2023. Table 1 below details the sources of each dataset.

Year	Source	Date Accessed
2017	File acquired from client: *LRSE_HPMSBin_Data_Cy2017_evw_2024-3-13(2002-2003 access format).mdb*	3/15/2024
2018	dTIMS BA Table: *GIS_CONDITION_CURRENT_YR_M4*	3/21/2024
2019	dTIMS BA Table: *GIS_CONDITION_CURRENT_YR_M3*	3/21/2024
2020	dTIMS BA Table: *GIS_CONDITION_CURRENT_YR_M2*	3/21/2024
2021	dTIMS BA Table: *GIS_CONDITION_CURRENT_YR_M1*	3/21/2024
2022	dTIMS BA Table: *GIS_CONDITION_CURRENT*	3/26/2024
2023	File acquired from client: *2023_DistressDelivery_02272024.gdb*	3/15/2024

Table 1: Yearly condition data sources and dates accessed

Each table mentioned above contains condition-based columns named as follows:

- AC_JPCPFC_CRCPFC_PMSCrackingPct
- AvgIRI

- HPMS_Cracking
- JPCP_JPCPFC_MaxFaultingHeight
- JPCP_JPCPFC_MeanFaultingHeight
- MaxRutting
- Rutting

An important aspect of the data is *when* the condition was measured. This knowledge allows Deighton to identify whether a treatment occurred before or after the condition was taken. Table 2 below details which column in which table contained 'data date' information, and the quality of the data.

Year	# of Rows	Column	% Blank	# Outside Data Year
2017	134,130	COLLECTION_DATE	97.51%	0
2018	136,582	DATADATE	0%	3,519
2019	140,455	DATADATE	0%	3,458
2020	138,739	DATADATE	0%	0
2021	153,615	DATADATE	0%	0
2022	143,411	DATADATE	0%	0
2023	116,704	COLLECTION_DATE	0%	0

Table 2: Breakdown of 'date collected' columns in each yearly condition file, including the % blanks and number of dates outside of its file's data year

As shown in the table, a few points in the 2017 data had collection date information (97.51% blank). The rest of the data years (2018-2023) had no blank values. However, there were a small number of dates that fell out of the expected date range. 2018 and 2019 had 3,519 and 3,458 dates outside of their data years, respectively.

2.1.2 Inventory Data

Other types of information detailing the pavement sections existing in dTIMS BA was used in the analysis. This data provides additional information for road segments in the condition data tables.

Table 3 below details each of the 'inventory tables' that were used for this analysis.

Inventory Type	**Source**	**Attribute(s) Used**
Constructed Year	dTIMS BA Table: *GIS_INVENTORY_CONSTRUCTED*	RoadName, From, To YearLastConstructed
Functional Class	dTIMS BA Table: *GIS_INVENTORY_FUNC_CLASS*	RoadName, From, To Functional_Class
Foundation Issues	dTIMS BA Table: *PMS_FOUNDATION_ISSUES*	RoadName, From, To Foundation_Issue
NHS	dTIMS BA Table: *GIS_INVENTORY_NHS*	RoadName, From, To NHS
Speed Limit	dTIMS BA Table: *GIS_INVENTORY_SPEED_LIMIT*	RoadName, From, To SpeedLimit
Terrain Type	dTIMS BA Table: *GIS_INVENTORY_TERRAIN*	RoadName, From, To TerrainType
Pavement Type	dTIMS BA Table: *PMS_PAVEMENT*	RoadName, From, To Pavement_Type
Seasonal Variation	dTIMS BA Table: *PMS_SEASONAL_VARIATION*	RoadName, From, To Seasonal_Variation
Traffic	File acquired from Client: *VPMS_TRAFFIC-2022.mdb*	RoadName, From, To AADT ESAL20
Minor Treatments	dTIMS BA Table: *PMS_PECOS*	RoadName, From, To ActivityDescription Date
Major Treatments	dTIMS BA Table: *PMS_PROJECT_HISTORY*	RoadName, From, To Completed

Table 3: Types of Inventory data used in the analysis, their sources, and the attributes used in each

2.2 Condition/Inventory Compilation

The first step of the compilation was to compile the yearly condition data available for each section. This way, the condition progression for each segment could be assessed. To append the yearly data, the sections found in the 2022 condition data were used to find direct matches in all other tables.

Following this, each section (unique combination of road name, from, and to attributes) was enriched with the following attributes from the inventory data (see section 2.1.2):

- *YearLastConstructed*
- *Functional_Class*
- *NHS*
- *SpeedLimit*
- *TerrainType*
- *Foundation_Issue*
- *Pavement_Type*
- *Seasonal_Variation*
- *AADT*
- *ESAL20*

To assign the 2022 sections with inventory data, the following process was implemented:

1. Check for a matching inventory section (inventory record fully overlaps with the section)
2. Check for semi matching inventory section (inventory record overlaps with *part* of the section)

Note: If multiple records overlapped with numerical data, the average of them was taken. If numerical aggregation couldn't be performed, the most recent property was taken.

Figure 1 below shows a visual representation of how the data will be handled.

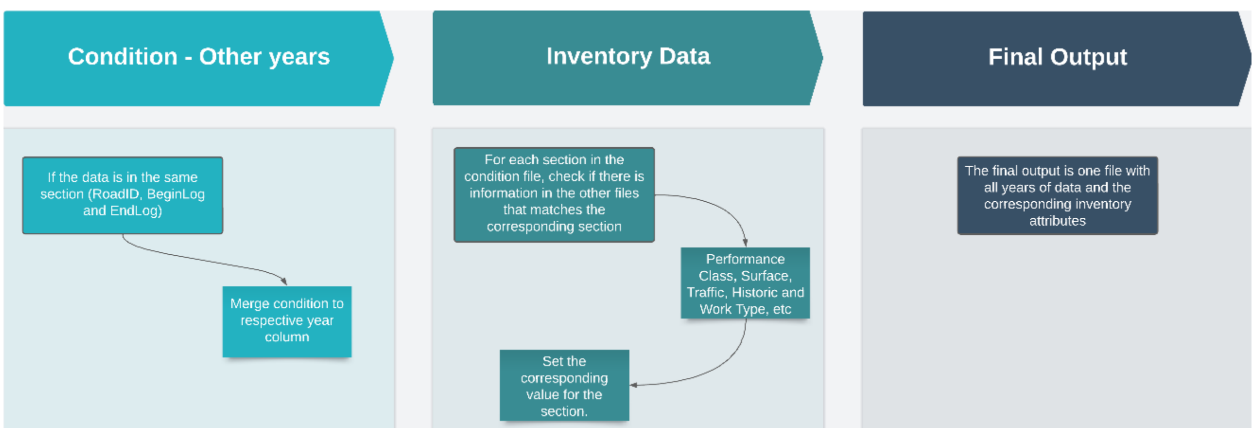

Figure 1: Data Processing process for Condition and Inventory data

If a match is found, the section inherits the value from the inventory table. Otherwise, the section's attribute is left blank.

The outcome is one record that contains the tenth-mile segmentation, all relevant inventory data, and all years of condition data for each distress. Table 4 below outlines attributes that are associated with each record after the data compilation process is completed.

2022 Sections	Inventory	Condition Values	Measured Dates
Road Name From To	YearLastConstructed Functional_Class NHS Speed Limit Terrain Type Foundation Issue Pavement Type Seasonal Variation AADT ESAL20	Condition_2017 Condition_2018 Condition_2019 Condition_2020 Condition_2021 Condition_2022 Condition_2023	DATADATE_2017 DATADATE_2018 DATADATE_2019 DATADATE_2020 DATADATE_2021 DATADATE_2022 DATADATE_2023

Table 4: List of attributes for each record following the Condition/Inventory compilation process

2.3 Recognized Treatment Resets

An important component of the analysis is identifying where and when significant improvements to condition occur in the network. After a treatment is completed, an improvement is expected soon thereafter. Deighton used the PMS_PECOS and PMS_PROJECT_HISTORY inventory tables mentioned in section 2.1.2 for minor and major treatment data respectively.

The minor treatment 'PECOS' includes treatments that ADOT considers don't impose a considerable reset in the condition of the roads. Only records with the following values in the 'ActivityDescription' field were considered:

- CRACK SEAL
- CONTRACT PAVEMENT MILLING & REPLACEMENT
- CONTRACT PAVING
- CONTRACT PAVEMENT PROFILING
- BITUMINOUS SURFACE SEAL

The date corresponding to each treatment was acquired from the 'Date' column PMS_PECOS.

All treatments from the PMS_PROJECT_HISTORY table are considered significant. The 'Completed' field in the PMS_PROJECT_HISTORY table was used as the completion date.

The significant treatment records were then compiled into one table (see Table 5 below). Each record in this custom lookup has an activity description, road name, from, to, completion date. The source table was included for reference.

RoadName	From	To	Activity Description	Date	Source Table
I008	0.694	0.894	CRACK SEAL	1/15/2020	PECOS
U1802	0	2.77012	NULL	2/1/1966	PROJECT_HISTORY
UY1910	1.315	3.49	CST NEW ROADWAY E OF EXIST	8/17/2005	PROJECT_HISTORY

Table 5: Sample of compiled PMS_PECOS and PMS_PROJECT_HISTORY data

2.4 Pavement Family Determination

Each road segment can be assigned a pavement family after it has been enriched with inventory data. To determine a pavement family, the following values are needed:

- Pavement Type
- Seasonal Variation Factor
- $ESALs_{20}$ *(equivalent standard axle loads for a design period of 20 years)*
- Foundation Issues

Table 6 below breaks down the pavement family code convention.

Pavement Type	**Climate (SVF)**	**ESALS**	**Foundation**
1- Asphalt 2- Composite 3- Concrete	1- Moderate 2- Severe	1- Very Low 2- Low 3- Moderate 4- High 5- Very High	1- Good 2- Poor

Table 6: Pavement type, climate, ESAL, and foundation code components of pavement families

The Pavement type code was determined using the following mapping for 'Pavement Type' column:

- BITUMINOUS - (Asphalt)
- AC OVERLAY OVER EXISTING JOINTED CONCRETE PAVEMENT - (Composite)
- JPCP - JOINTED PLAIN CONCRETE PAVEMENT - (Concrete)

The Climate type can be categorized using the 'Seasonal_Variation' attribute according to Table 7 below.

Climate Categories based on SVF		
Moderate	0.00	1.50
Severe	1.50	5.00

Table 7: SVF categories for pavement family determination

Similarly, the ESAL category of the 'ESAL' attribute is categorized using Table 8 below.

$ESALs_{20}$Categories	**Minimum $ESALs_{20}$**	**Maximum $ESALs_{20}$**
Very Low	-	300,000
Low	300,000	3,000,000
Moderate	3,000,000	10,000,000
High	10,000,000	30,000,000
Very High	30,000,000	-

Table 8: $ESALs_{20}$ categories for pavement family determination

The Foundation category was determined using the 'Foundation_Issue' attribute:

- 'Y' – Poor
- Otherwise – Good

2.5 Data Cleaning

The objective of cleaning the deterioration data is to reduce the negative impact of 'bad data' on subsequent analysis stages.

Data to be used within the deterioration curve development needed to be investigated for suitability prior to being included within any statistical analysis. The filtering and cleaning process investigates the data so that any outliers are excluded. For example:

- Segments with missing pavement family categories (see section 2.4).
- Segments with extraordinary deterioration will be excluded.
- Points within segments that have no past condition resets were excluded (see section 2.3).
- Points within segments that aren't part of a valid condition run were excluded (section 2.5.1).

An overview of the data and the results of the data cleaning process is given in Table 9 below.

Condition-Inventory Table	Rows	Incomplete Family Code Rows	% Valid Condition Points	# Condition Points	# Condition Points Removed
AC_JPCPFC_CRCPFC_PMSCrackingPct	148,190	33,246	77.72%	806,208	464,026
AvgIRI	148,236	33,248	78.55%	815,093	421,104
HPMS_Cracking	148,191	33,246	78.68%	816,177	487,774
JPCP_JPCPFC_MaxFaultingHeight	148,078	33,245	2.91%	30,149	10,292
JPCP_JPCPFC_MeanFaultingHeight	148,078	33,245	2.91%	30,159	11,132
MaxRutting	148,236	33,248	77.83%	807,584	571,399
Rutting	148,236	33,248	77.83%	807,584	548,361

Table 9: Condition/Inventory table data cleaning summary with number of condition points lost

The columns in the table are described as follows:

- The 'Rows' column lists how many rows (segments) were compiled.
- The 'Incomplete Family Code Rows' column shows how many Pavement Family codes were missing one of four required categories (i.e., ESAL, SVF, Foundation, or Pavement Type).
- Then, the '% Valid Condition Points column' lists the percentage of condition points that were valid out of the possibly valid ones (7 for each segment).
- The number of condition points is also expressed in the next column.
- Finally, the number of condition points removed in the Deterioration Run Analysis stage (section 2.5.1) is listed.

2.5.1 Deterioration Run Analysis

Deighton analyzed the deterioration behavior of each segment over time and removed data that didn't follow deterioration patterns aligning with known ADOT treatment records.

The validity of the next condition point can be assessed using:

- The next year's condition.
- Dates of performed treatments (section 2.3).
- The date the condition was recorded (DATADATE columns) (section 2.2).

A point is considered invalid if it is an improvement relative to the last measured point and has no treatment to explain it. The logic for this process is as follows:

1. If the next point is an improvement in condition greater than 5% relative to the first, check if there is a treatment between the first and second point.
    a. If there is a treatment, the next point would represent the beginning of a deterioration run
    b. If there is no treatment, the next point is discarded and is considered erroneous. Points are discarded until a treatment explains an improvement relative to the original point, or the point is no longer an improvement relative to the original point.

Figure 2 below shows an example of the deterioration logic, where a valid string of deterioration is observed from points 0 -3. After point 3, an improvement is observed. The time frame between the two points is checked for a treatment. In this case, no treatments are in the records. Because of this, the next valid point is point 7, which is no longer an improvement relative to point 3.

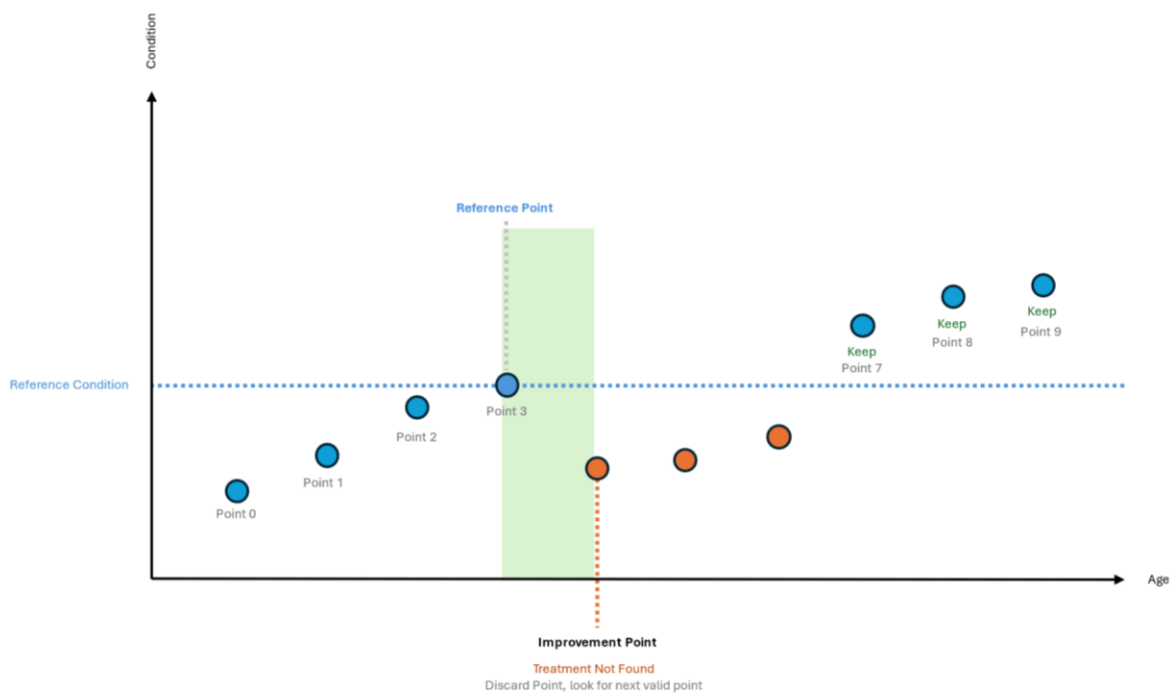

Figure 2 – Example of deterioration improvement logic, where an improvement not supported by treatment data is encountered

2.6 Age Determination

In conjunction with the treatment data section 2.3, the age – how old the road segment was at the time of the measured condition can be calculated.

Three columns are used to calculate the age of the first condition point of a segment:

- Significant Minor Treatments
- Major Treatments
- Year_Last_Constructed

The most recent date between them, relative to the first condition point in the set (i.e., 2017) is used as an effective birthday of the segment. All points before the effective birthday will be regarded as invalid data (see section 2.5) Progressing through the condition points (i.e., through 2023), the age is reset if an improvement in condition is found AND a treatment date is found prior. Table 10 below details the number of condition points that were removed due to there being no discernable age.

Condition-Inventory Table	Condition Points	Total Condition Points Removed	Condition Points Removed (No Age)
AC_JPCPFC_CRCPFC_PMSCrackingPct	806,208	464,026	187,147
AvgIRI	815,093	421,104	209,478
HPMS_Cracking	816,177	487,774	173,473
JPCP_JPCPFC_MaxFaultingHeight	30,149	10,292	1,575
JPCP_JPCPFC_MeanFaultingHeight	30,159	11,132	1,798
MaxRutting	807,584	571,399	124,070
Rutting	807,584	548,361	134,845

Table 10: Number of condition points removed for each condition variable due to there being no discernable age

3 Analyzing Current Models

Before conducting a statistical analysis of pavement families and condition data to develop new families and deterioration models, it was essential to assess the effectiveness of the original models. Deighton evaluated these models by predicting pavement deterioration and comparing the predictions to actual deterioration for each distress type and pavement family.

This evaluation is crucial because new data is available, and it is necessary to determine if the existing models can accurately predict this new data. If the models are not accurate, adjustments or new models may be needed.

The evaluation process involved plotting data points on a Cartesian plane, with the predicted values from the original models on the y-axis and the actual collected values on the x-axis. A 45-degree line was then drawn on the graph, representing perfect agreement between predictions and actual values.

By plotting all data points, one can regress a line through the points and compare it to the 45-degree line. If the regression line is above the 45-degree line, it indicates that the predictions are generally higher than the actual values. Conversely, if the regression line is below the 45-degree line, it means the predictions are generally lower than the actual values.

For example, consider the data shown in Figure 3. It uses collected rutting data and existing models to predict rutting. The graph shows that the blue line (predicted values) is below the orange line (actual values), indicating that the data points are underpredicting the actual observed deterioration.

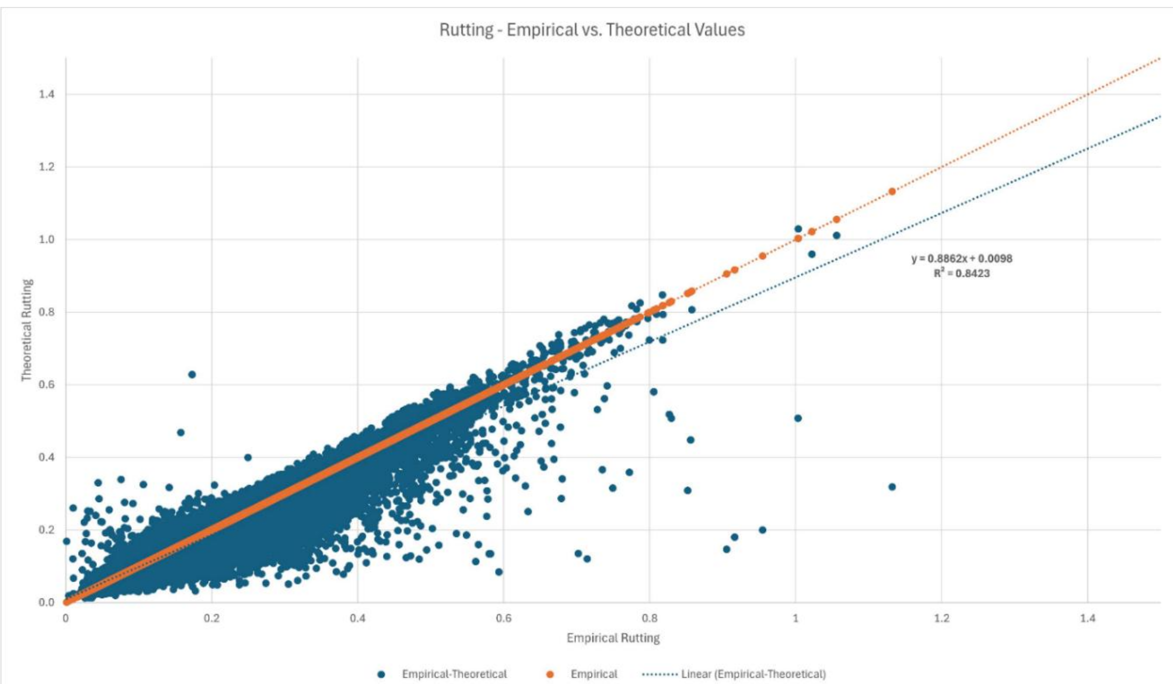

Figure 3: Predicted IRI vs Actual IRI

Deighton performed this for each condition variable's condition data. These provided the needed input to assess that a re-evaluation of the curves was indeed needed and warranted. The individual results can be found in Appendix A which showcases the results of this analysis.

4 Analyzing Family of Curves

Homogeneous performance families were originally generated using engineering assessment and statistical analysis in cooperation with ADOT.

The previous analysis determined the following attributes to define families of curves:

- Pavement construction type (flexible, rigid, semi-rigid).
- Foundation quality (good or poor).
- Traffic volume (expressed by ESAL20s).
- Climate information (moderate or severe).

The family of curves were analyzed to evaluate how different attributes display a tendency of deterioration. Deighton evaluated the inclusion of other variables in the analysis to determine if any additional attributes would provide significant statistically proven implications. Sub-categories such as traffic levels, soil strength, and functional class were established for each attribute. A count was then conducted for each sub-category to determine the number of sections with index variations and the magnitude of the change.

4.1 Statistical Analysis

In the statistical analysis, different processes were carried out to analyze the correlation between different dependent and independent variables to assess the hypothesis on the homogeneous performance families and to analyze the difference between data points as a basis for definition. Finally, statistical assessment of the postulated hypotheses on deterministic deterioration functions were performed. The following items were considered, developed, and reported:

- Correlation matrix of the different dependent and independent variables using the yearly "delta" of the technical parameters (condition attributes) between data points for each pavement family.
- Analysis of variance (ANOVA) to assess the dependencies of the different homogeneous performance families considering the null hypothesis that the means are equal.
- Descriptive statistical analysis of delta values with 80% sample of the data (20% will be used to test the postulated hypotheses on deterministic deterioration functions).
    - Calculation of the yearly "delta" of the technical parameters between the data points for each homogeneous performance family.
    - Descriptive statistical analysis of the yearly "delta" values for each performance family.

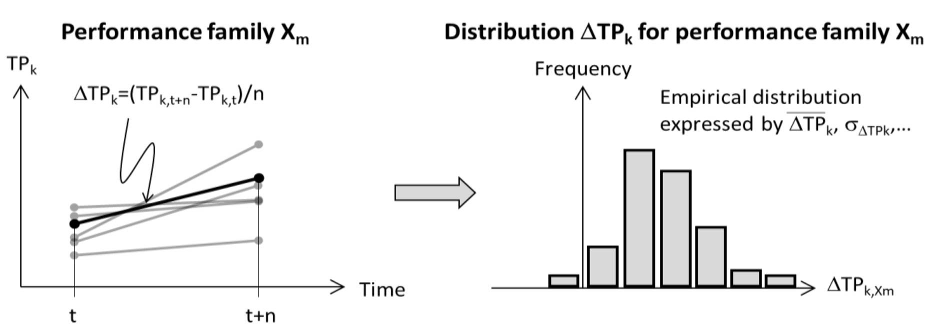

Figure 4: Calculation of Yearly "delta" (schematically) and descriptive statistical analysis

An example of how families are evaluated is displayed in Figure 5. This graph shows the difference in rutting from 2017 to 2018 for each section of the road with condition data, in this case at a tenth mile level, distributed by ESAL code (1 to 5) and further split into ranges.

For example, if a road with ESAL code 2 had a variation of 0.14 in rutting, it would be counted towards the orange group.

The label on the vertical axis represents the rate of change of the condition being evaluated, with the percentages indicating the amount of sections of a road that changed within a certain range. In this example, the ranges are:

- 0 - 0.025
- 0.025 - 0.05
- 0.05 - 0.075
- 0.075 - 0.1
- 0.1+

Each data point corresponds to one section of a road that has data for one year, and the next year, the difference in condition from one year to the other is calculated as one individual record. This process is repeated for every year and every section of all roads available.

This graph illustrates how deterioration ranges change based on ESAL code. In this example, we see that the ESAL code significantly impacts the distribution: 27.5% of roads with ESAL code 3 have a change greater than or equal to 0.1, while 59.1% of roads with ESAL code 5 have a change greater than 0.1. Thus, ESAL is significant in evaluating how deterioration occurs.

This analysis was conducted for all selected attributes, all years with available data, and all conditions. The individual results can be found in Appendix B: Analyzing Family of Curves showcases the results of this analysis. From this, Deighton once again confirmed that ESAL, Pavement Type, Seasonal Variation Factor, and Foundation Issues are significant factors to be used as family generators.

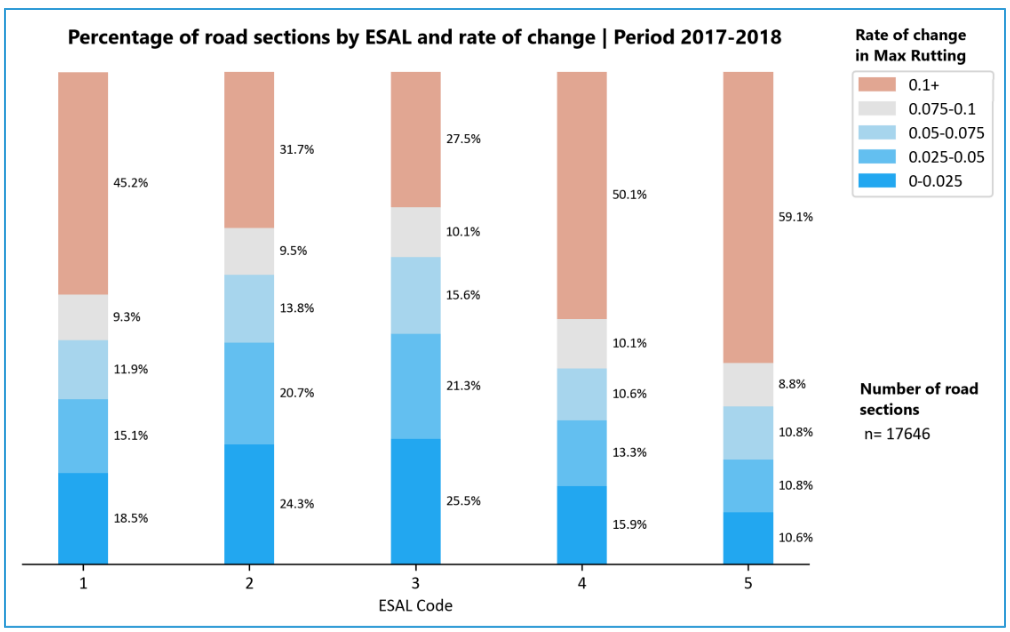

Figure 5: Example of ESALS impact on Max Rutting

5 Deterioration Curves

After the families were confirmed, Deighton moved forward with the analysis of specific curves for each defined family. The model will utilize the sets of variables defined on the family of curves evaluation to calculate the condition.

5.1 Methodology

The general deterioration functions to be calculated were based on a deterministic approach, which calculates the yearly value of the condition parameter subject to the different influencing factors. Machine learning algorithms are used to determine the different model parameters (coefficients) to best match the condition data to each pavement family.

Different types of equations were calculated to evaluate which one suits the deterioration of each given family. Then, the curves were compared, and the best accuracy will be determined based on a calculation of the mean average error.

5.2 Outliers

Outliers were calculated using the whole sample remaining after data transformation and cleansing (sections 2.5 and 2.5.1 in the document). Ultimately, data within a Pavement Family will have a myriad of condition-age points.

Within each pavement family, the mean and standard deviation were calculated for each age. To account for errors in the data, varying upper and lower tolerance (allowed standard deviations from the mean) was used to identify outliers. If the condition was above the age's mean, the upper tolerance (σ_{upper}) was used. Otherwise, the lower tolerance (σ_{lower}) was used. Table 11 below exemplifies the variation in tolerance as age increases – the upper tolerance is increased by 5% of the standard deviation each year. The lower tolerance remains fixed at 0.5 standard deviations.

Age	σ_{upper}	σ_{lower}
1	1.05	0.5
2	1.1	0.5
3	1.15	0.5
4	1.2	0.5
5	1.25	0.5
6	1.3	0.5
7	1.35	0.5
8	1.4	0.5
9	1.45	0.5
10	1.5	0.5

Table 11: Upper/lower condition tolerances (in terms of standard deviations) at each age used to determine outliers

Outliers will be kept in the data displayed but will not be used for generating the curves (see Section 6 for more details).

5.3 Curve Equations

Following the outlier determination, curve regression was performed. All curves – or equations – were generated considering non-outlier data for each pavement family. The following curve types were selected to represent real-world trends in pavement condition most accurately:

- **Linear:** $a \cdot x + L$
- **Quadratic:** $a \cdot x^2 + L$
- **Exponential:** $a \cdot e^{b \cdot x} + L$

In the equations above, *a* and *b* represent parameters optimized during regression. *L* is the parameter required to ensure the equation begins at a desired value at age 0 (i.e., the initial deterioration at age 0). This value varies depending on the deterioration index being evaluated (i.e., average IRI, percent cracking...). For all indexes, the initial deterioration was set to 0. In the case of IRI, the initial deterioration was set to 45.

5.4 Curve Fitting Methodology

The method of least squares was used to generate the optimal parameters in the equations discussed above. The technique operates by reducing (or minimizing) the differences between the data (condition-age points) and the resultant fitted curve. This minimization was conducted at each age value on the x-axis. Figure 5 below visualizes fundamentals of *linear* curve fitting for reference.

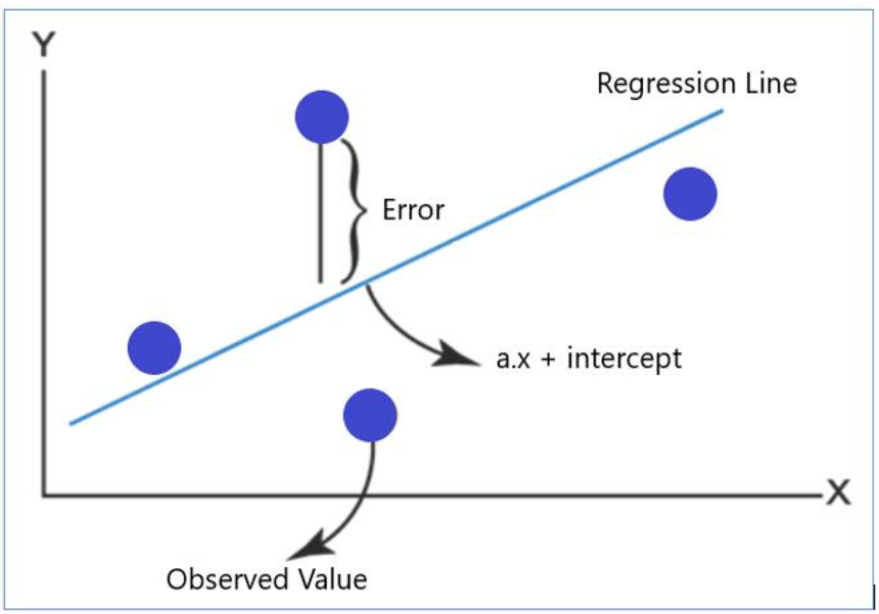

Figure 5: Least Squares Optimal Fit Method

In the case of *quadratic* and *exponential* curve fitting, the same technique of minimizing error between the data and the fitted curve was employed. The accuracy of each generated curve from an error perspective is detailed in Section 5.5.

5.5 Error Evaluation

As mentioned above, the curve fitting process was guided by minimizing error at each age. The optimal solution was given in the form of optimal equation parameters (i.e., a, b, L). To converge on this optimal solution, the Mean Absolute Error (MAE) was calculated for each curve – quantifying the average size of the errors in a group of predictions. This error is agnostic to the nature of error, disregarding if the forecasted curve was overpredicting or underpredicting. Therefore, it can be used as a measure of how much the forecasted curve deviated from the data on average.

The equation below represents the MAE:

$$MAE = \frac{\sum_1^n |\gamma_i - y_i|}{n}$$

Where:

- γ_i represents the predicted condition at an age.
- y_i is the actual condition observed in the data.
- n is the total number of data points.

5.6 Curves Eliminated from Analysis

Curves showing improvement in deterioration were disregarded, ensuring the overall trend remains towards deterioration. For instance, all the ADOT distresses slope upward, so any downward trending curves will be ignored.

6 Results

The results of the Deterioration Analysis were a series of equations for five different pavement deterioration indices and the different pavement families within them. These results were visualized on interactive dashboards that powered discussion between Deighton and ADOT.

Ultimately, the equations were input into dTIMS BA and the Analysis Set used by ADOT was updated. The sections to follow break down the details of the result set.

6.1 Curve Selection Process

After generating the curves for each family and index, Deighton recommended the ideal curves to implement in dTIMS BA. These recommendations consider not only mathematical accuracy based on the mean average error but also the shape of the curves, as identified by our pavement experts for predicting pavement deterioration.

In some cases, the quality/quantity of the data prevented accurate curve generation during the curve fitting process. To provide the most accurate forecasts in lieu of data, Deighton sourced curves using two different methodologies:

- **Replace curves from closely related families**
  Related curves were chosen by varying ESAL codes, then, SVF, then Foundation Issues, respectively. Replacement curves were never selected from families with different Pavement Types (excluding family '3000').
- **Generate new curves using available statistics**
  New curves were generated if the above method was not suitable due to variations in family behavior. Using the expertise of pavement experts and the performance of previous curves (see Appendix A: Analyzing Current Models) new curves were generated.

For example, if a family was lacking data, similar families with data were used if suitable. If not, the previous curve and its performance compared to empirical data was assessed. If the previous curve was under-forecasted, a new curve was generated that under-forecasted slightly less compared to it. This process was also improved by enforcing expected deterioration patterns.

Following review of the dashboard, Deighton applied a small scaling factor to the equation's coefficients. For this reason, the coefficients of equations in the dTIMS BA setup will vary slightly from the ones shown in the dashboard.

The following section will detail the selected curves. Please note, extended results including equations can be viewed in the Dashboards (see section 6.4).

6.2 Selected Curves

Using the selection process in section 6.1, Deighton provided ADOT with deterioration curves. The following tables show the curve types generated for each condition index and family within them. The Description field specifies the source of each equation and contains the following:

- "Good Data" indicates the curve was generated directly from ADOT's data.
- "Matched To" indicates the family used another family's curve.
- Custom indicates a curve was generated by Deighton using available statistics and insights.

Table 12 below displays the results of the Average IRI curve fitting process. The data available for Average IRI resulted in plenty of successful curve fittings.

Note: Family '3000' represents all families beginning with '3'.

Condition Index	Family	Equation Type	Description
Average IRI	1111	Linear	Good Data
Average IRI	1112	Quadratic	Good Data
Average IRI	1121	Linear	Matched to 1121
Average IRI	1122	Quadratic	Matched to 1132
Average IRI	1131	Exponential	Good Data
Average IRI	1132	Quadratic	Good Data
Average IRI	1141	Quadratic	Good Data
Average IRI	1142	Quadratic	Matched to 1132
Average IRI	1151	Linear	Good Data
Average IRI	1152	Quadratic	Matched to 1132
Average IRI	1211	Linear	Matched to 1221
Average IRI	1212	Linear	Matched to 1112
Average IRI	1221	Linear	Good Data
Average IRI	1222	Quadratic	Matched to 1132
Average IRI	1231	Linear	Matched to 1221
Average IRI	1232	Quadratic	Matched to 1132
Average IRI	1241	Quadratic	Matched to 1132
Average IRI	1242	Quadratic	Matched to 1132
Average IRI	1251	Quadratic	Matched to 1132
Average IRI	1252	Quadratic	Matched to 1132
Average IRI	2111	Linear	Matched to 2241
Average IRI	2112	Exponential	Custom
Average IRI	2121	Quadratic	Matched to 2151
Average IRI	2122	Exponential	Custom
Average IRI	2131	Quadratic	Matched to 2151
Average IRI	2132	Exponential	Custom
Average IRI	2141	Quadratic	Matched to 2151
Average IRI	2142	Exponential	Custom
Average IRI	2151	Linear	Good Data
Average IRI	2152	Linear	Matched to 2151
Average IRI	2211	Linear	Matched to 2241
Average IRI	2212	Exponential	Custom
Average IRI	2221	Linear	Matched to 2241
Average IRI	2222	Exponential	Custom
Average IRI	2231	Linear	Matched to 2241
Average IRI	2232	Linear	Matched to 2241
Average IRI	2241	Linear	Good Data
Average IRI	2242	Exponential	Custom
Average IRI	2251	Quadratic	Good Data
Average IRI	2252	Quadratic	Matched to 2251
Average IRI	3000	Linear	Matched to 2151

Table 12: Average IRI curve selection results

Table 13 below shows the curve fitting results for Cracking Percent.

Condition Index	Family	Equation Type	Description
Cracking Percent	1111	Quadratic	Good Data
Cracking Percent	1112	Quadratic	Matched to 1132
Cracking Percent	1121	Quadratic	Good Data
Cracking Percent	1122	Quadratic	Matched to 1132
Cracking Percent	1131	Quadratic	Good Data
Cracking Percent	1132	Quadratic	Good Data
Cracking Percent	1141	Quadratic	Good Data
Cracking Percent	1142	Quadratic	Matched to 1132
Cracking Percent	1151	Quadratic	Good Data
Cracking Percent	1152	Quadratic	Matched to 1132
Cracking Percent	1211	Quadratic	Good Data
Cracking Percent	1212	Exponential	Custom
Cracking Percent	1221	Quadratic	Good Data
Cracking Percent	1222	Exponential	Custom
Cracking Percent	1231	Quadratic	Good Data
Cracking Percent	1232	Exponential	Custom
Cracking Percent	1241	Linear	Good Data
Cracking Percent	1242	Exponential	Custom
Cracking Percent	1251	Linear	Good Data
Cracking Percent	1252	Linear	Good Data
Cracking Percent	2111	Linear	Good Data
Cracking Percent	2112	Quadratic	Custom
Cracking Percent	2121	Quadratic	Matched to 2141
Cracking Percent	2122	Quadratic	Custom
Cracking Percent	2131	Quadratic	Matched to 2141
Cracking Percent	2132	Quadratic	Custom
Cracking Percent	2141	Quadratic	Good Data
Cracking Percent	2142	Quadratic	Custom
Cracking Percent	2151	Linear	Good Data
Cracking Percent	2152	Quadratic	Custom
Cracking Percent	2211	Quadratic	Matched to 2241
Cracking Percent	2212	Quadratic	Custom
Cracking Percent	2221	Quadratic	Matched to 2241
Cracking Percent	2222	Quadratic	Custom
Cracking Percent	2231	Quadratic	Matched to 2241
Cracking Percent	2232	Quadratic	Custom
Cracking Percent	2241	Quadratic	Good Data
Cracking Percent	2242	Quadratic	Matched to 2241
Cracking Percent	2251	Quadratic	Good Data
Cracking Percent	2252	Quadratic	Matched to 2252
Cracking Percent	3000	Quadratic	Matched to 2252

Table 13: Cracking Percent curve selection results

The quality of data available resulted in successful curve fitting in most cases. In areas where Deighton could not fit curves to the data, custom curves were generated using the processes detailed in section 6.1.

Table 14 below shows the results of the HPMS Cracking curve fitting process.

Condition Index	Family	Equation Type	Description
HPMS Cracking	1111	Quadratic	Good Data
HPMS Cracking	1112	Quadratic	Custom
HPMS Cracking	1121	Quadratic	Matched to 1111
HPMS Cracking	1122	Quadratic	Custom
HPMS Cracking	1131	Quadratic	Good Data
HPMS Cracking	1132	Quadratic	Custom
HPMS Cracking	1141	Quadratic	Good Data
HPMS Cracking	1142	Quadratic	Custom
HPMS Cracking	1151	Quadratic	Good Data
HPMS Cracking	1152	Quadratic	Custom
HPMS Cracking	1211	Quadratic	Good Data
HPMS Cracking	1212	Quadratic	Good Data
HPMS Cracking	1221	Quadratic	Matched to 1211
HPMS Cracking	1222	Quadratic	Matched to 1212
HPMS Cracking	1231	Quadratic	Good Data
HPMS Cracking	1232	Quadratic	Matched to 1212
HPMS Cracking	1241	Quadratic	Good Data
HPMS Cracking	1242	Quadratic	Matched to 1212
HPMS Cracking	1251	Quadratic	Good Data
HPMS Cracking	1252	Quadratic	Good Data
HPMS Cracking	2111	Quadratic	Custom
HPMS Cracking	2112	Quadratic	Custom
HPMS Cracking	2121	Quadratic	Custom
HPMS Cracking	2122	Quadratic	Custom
HPMS Cracking	2131	Quadratic	Custom
HPMS Cracking	2132	Quadratic	Custom
HPMS Cracking	2141	Quadratic	Custom
HPMS Cracking	2142	Quadratic	Custom
HPMS Cracking	2151	Quadratic	Custom
HPMS Cracking	2152	Quadratic	Custom
HPMS Cracking	2211	Quadratic	Matched to 2221
HPMS Cracking	2212	Quadratic	Custom
HPMS Cracking	2221	Quadratic	Good Data
HPMS Cracking	2222	Quadratic	Custom
HPMS Cracking	2231	Quadratic	Matched to 2221
HPMS Cracking	2232	Quadratic	Custom
HPMS Cracking	2241	Quadratic	Matched to 2251
HPMS Cracking	2242	Quadratic	Custom
HPMS Cracking	2251	Quadratic	Good Data
HPMS Cracking	2252	Quadratic	Custom

Table 14: HPMS Cracking curve selection results

During this process, there was successful curve fitting for most pavement families beginning in 1 (i.e., 1XXX). There was limited quality data available for families beginning in 2 (i.e., 2XXX), in which case Deighton used domain knowledge and previous statistical results to derive suitable curves (see section 6.1 for details on this process).

Table 15 below shows the curve fitting results for Max Faulting.

Condition Index	Family	Equation Type	Description
Max Faulting	3111	Quadratic	Custom
Max Faulting	3112	Quadratic	Custom
Max Faulting	3121	Quadratic	Custom
Max Faulting	3122	Quadratic	Custom
Max Faulting	3131	Quadratic	Custom
Max Faulting	3132	Quadratic	Custom
Max Faulting	3141	Quadratic	Custom
Max Faulting	3142	Quadratic	Custom
Max Faulting	3151	Quadratic	Custom
Max Faulting	3152	Quadratic	Custom
Max Faulting	3211	Quadratic	Custom
Max Faulting	3212	Quadratic	Custom
Max Faulting	3221	Quadratic	Custom
Max Faulting	3222	Quadratic	Custom
Max Faulting	3231	Quadratic	Custom
Max Faulting	3232	Quadratic	Custom
Max Faulting	3241	Quadratic	Custom
Max Faulting	3242	Quadratic	Custom
Max Faulting	3251	Quadratic	Custom
Max Faulting	3252	Quadratic	Custom

Table 15: Max Faulting curve selection results

There was limited available data for all families in this deterioration index. As with other condition indices, Deighton used domain knowledge and previous statistical results to derive suitable curves (see section 6.1 for details on this process).

Table 16 below shows the results of the curve fitting process for Rutting.

Condition Index	Family	Equation Type	Description
Rutting	1111	Quadratic	Good Data
Rutting	1112	Quadratic	Custom
Rutting	1121	Quadratic	Good Data
Rutting	1122	Quadratic	Custom
Rutting	1131	Quadratic	Good Data
Rutting	1132	Quadratic	Custom
Rutting	1141	Quadratic	Good Data
Rutting	1142	Quadratic	Custom
Rutting	1151	Quadratic	Good Data
Rutting	1152	Quadratic	Custom
Rutting	1211	Quadratic	Good Data
Rutting	1212	Quadratic	Custom
Rutting	1221	Quadratic	Good Data
Rutting	1222	Quadratic	Custom
Rutting	1231	Quadratic	Good Data
Rutting	1232	Quadratic	Custom
Rutting	1241	Quadratic	Good Data
Rutting	1242	Quadratic	Custom
Rutting	1251	Quadratic	Good Data
Rutting	1252	Quadratic	Custom
Rutting	2111	Quadratic	Good Data
Rutting	2112	Quadratic	Custom
Rutting	2121	Quadratic	Good Data
Rutting	2122	Quadratic	Custom
Rutting	2131	Quadratic	Matched to 2132
Rutting	2132	Quadratic	Custom
Rutting	2141	Quadratic	Good Data
Rutting	2142	Quadratic	Custom
Rutting	2151	Quadratic	Good Data
Rutting	2152	Quadratic	Custom
Rutting	2211	Quadratic	Matched to 2251
Rutting	2212	Quadratic	Custom
Rutting	2221	Quadratic	Matched to 2251
Rutting	2222	Quadratic	Custom
Rutting	2231	Quadratic	Matched to 2251
Rutting	2232	Quadratic	Custom
Rutting	2241	Quadratic	Matched to 2251
Rutting	2242	Quadratic	Custom
Rutting	2251	Quadratic	Good Data
Rutting	2252	Quadratic	Custom

Table 16: Rutting curve selection results

The results for Rutting were deduced from curve fitting the data and generating custom curves. There were significant data gaps found which warranted doing so. As with other condition indices, Deighton used domain knowledge and previous statistical results to derive suitable curves (see section 6.1 for details on this process).

6.3 BA Implementation

Using the results of the curve fitting process, the dTIMS BA environment was ready to be modified and tested. The Analysis was first modified on Deighton's servers and the results were reviewed to ensure the accuracy of the new curves.

Following the first reviews, the curves were altered slightly to improve their performance – a modifier was applied that slightly decreased the deterioration rate. This decision was made at the recommendation of Deighton's pavement deterioration experts after reviewing the Analysis Sets.

The results were then reviewed again for accuracy by comparing them with previous distributions. Section 6.3.1 outlines the results of the good/fair/poor condition distributions across the network for different Budget Scenarios.

Based on the results of the Analysis Set and the good/fair/poor distributions for many Budget Scenarios, the recommended curves were implemented in that ADOT on-prem production version of dTIMS BA following the approval from ADOT on October 15th, 2024.

With the implementation of the new models in the ADOT on-prem dTIMS BA and the delivery of this report, the project is substantially complete with on-site training remaining.

6.3.1 Result Review

The figures below show the good, fair, and poor distributions of multiple Budget Scenarios before and after the curves were changed. It is important to note that these results are suitable for up to 25 years.

Figure 6 below shows the good/fair/poor distribution for the ‘Do Nothing' budget scenario for the previous curves and the new curves. The main difference between them was how fast the poor condition dominated the distribution. These results align with expectations – if pavement is left untreated, the poor condition will dominate the distribution at around 25 years.

Do-Nothing – Previous Curves

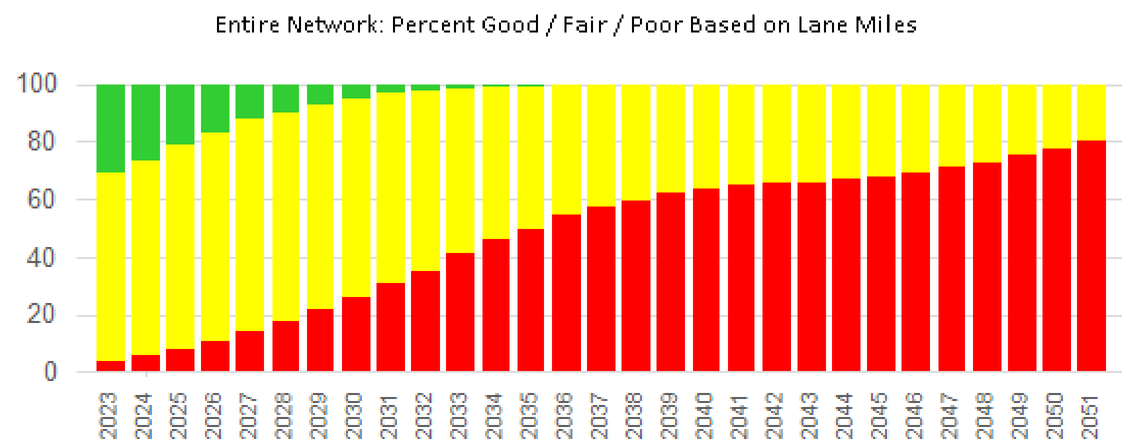

Do-Nothing – New Curves

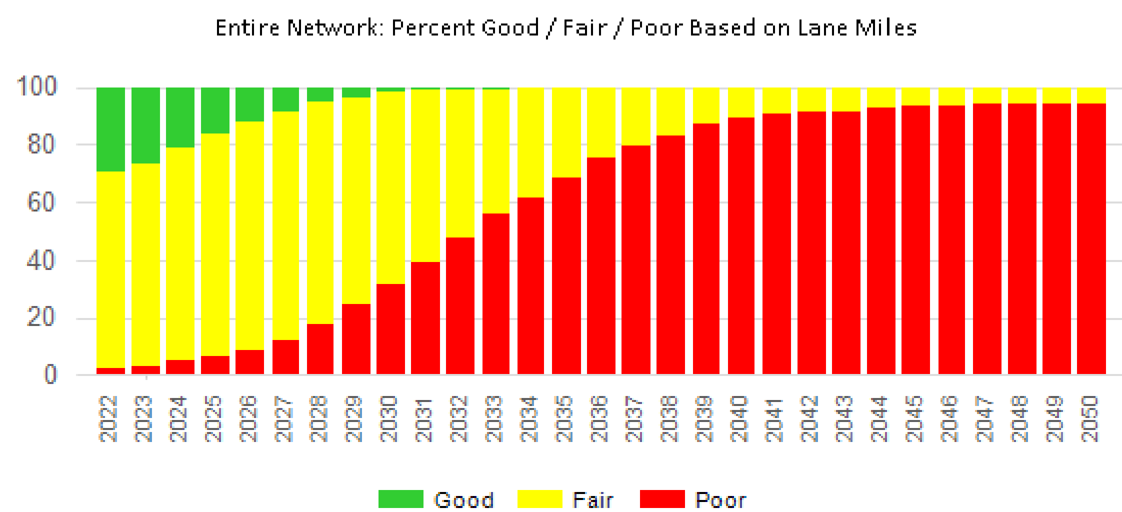

Figure 6: Comparison of condition distribution for the ‘Do Nothing’ scenario

Figure 7 below compares good/fair/poor distribution for the Unlimited budget scenario for previous and new curves. In the new results, the fair condition increased slightly in the early stages. Other than that, there were little significant changes, which is to be expected in this unlimited scenario.

Unlimited – Previous Curves

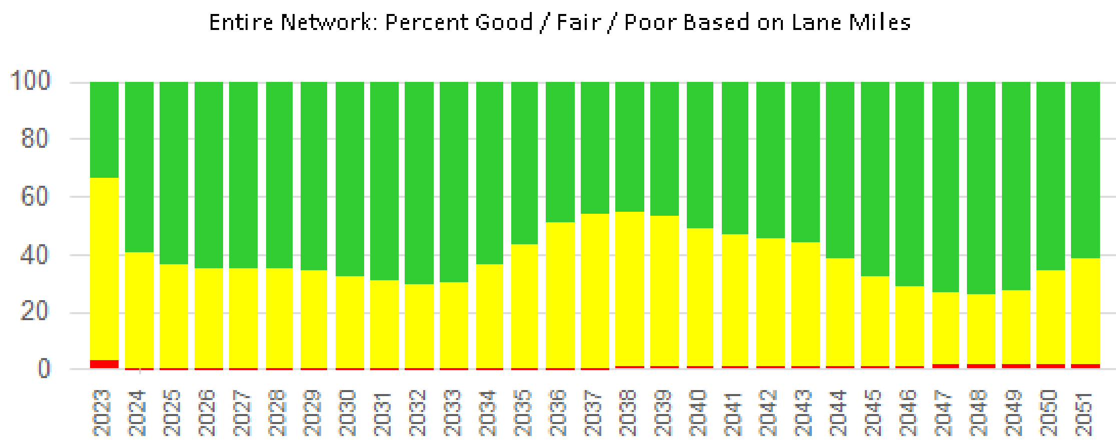

Unlimited – New Curves

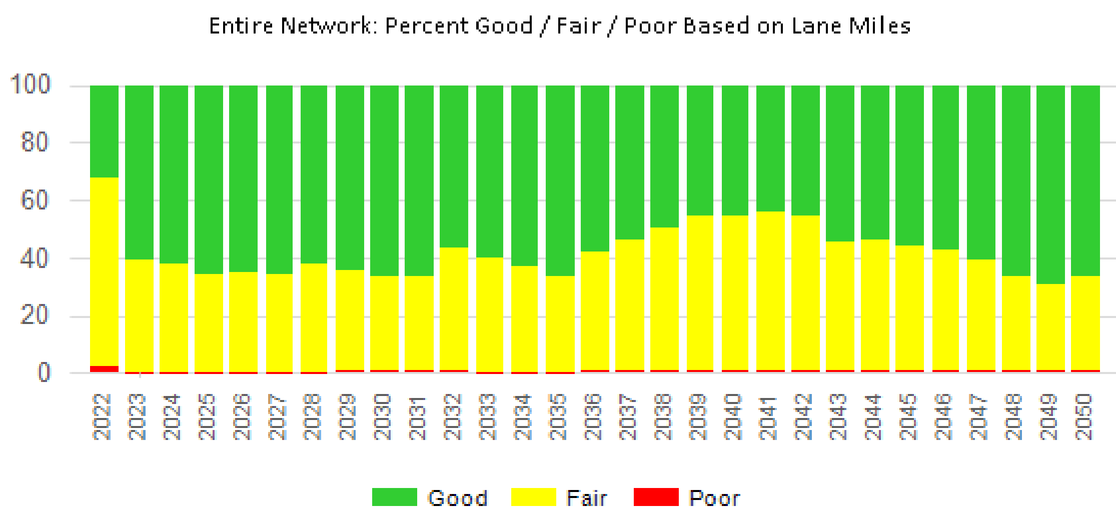

Figure 7: Comparison of condition distribution for the 'Unlimited' scenario

Figure 8 below compares good/fair/poor distribution for the ‘Budget 6’ budget scenario for previous and new curves. In the new scenario with updated curves, the poor condition increased slightly in the middle to late stages of the Analysis. This behavior was explained by the fact that deterioration rates increased. The distribution of fair condition also increased in the middle to late stages of the Analysis, which aligned with Deighton’s expectations.

Budget 6 – Previous Curves

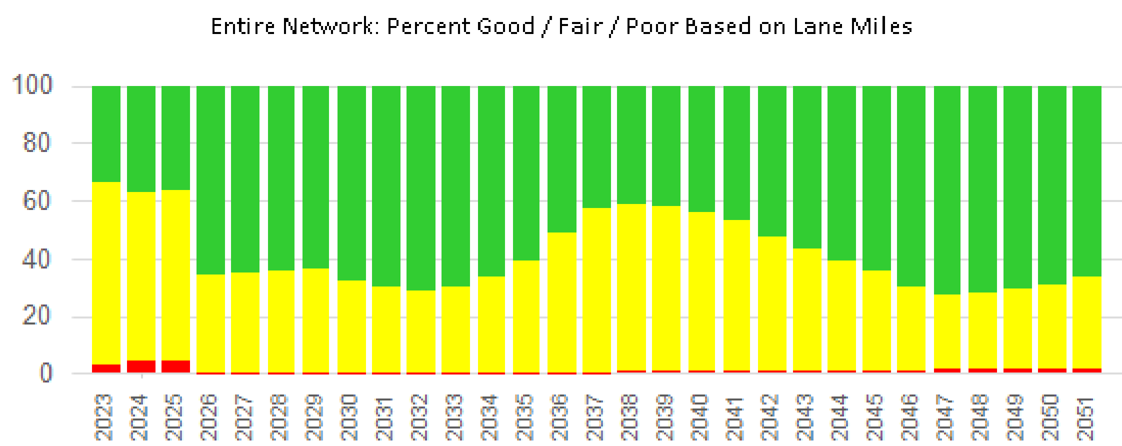

Budget 6 – New Curves

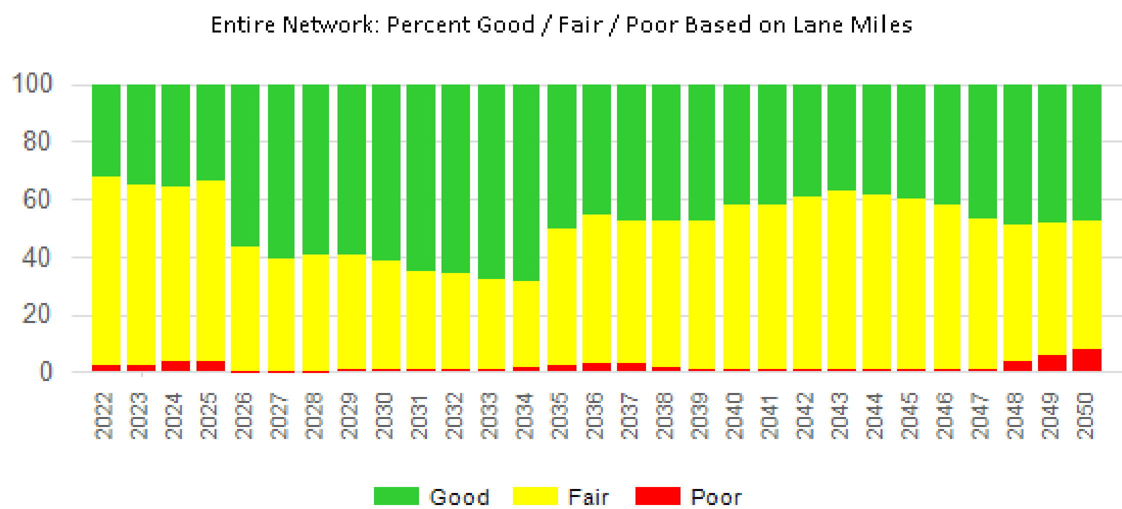

Figure 8: Comparison of condition distribution for the ‘Budget 6’ scenario

Figure 9 below compares good/fair/poor distribution for the 'Budget 8' budget scenario for previous and new curves. The results of this distribution aligned with Deighton's expectations. Given the deterioration rates generally increased compared to the previous curves, the increases in poor condition in the middle of the Analysis was expected and accurate behavior.

Budget 8 – Previous Curves

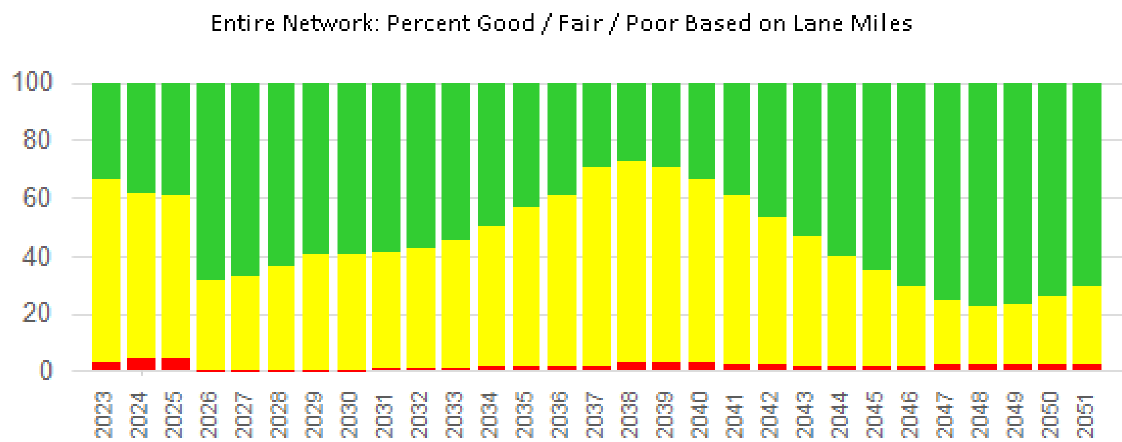

Budget 8 – New Curves

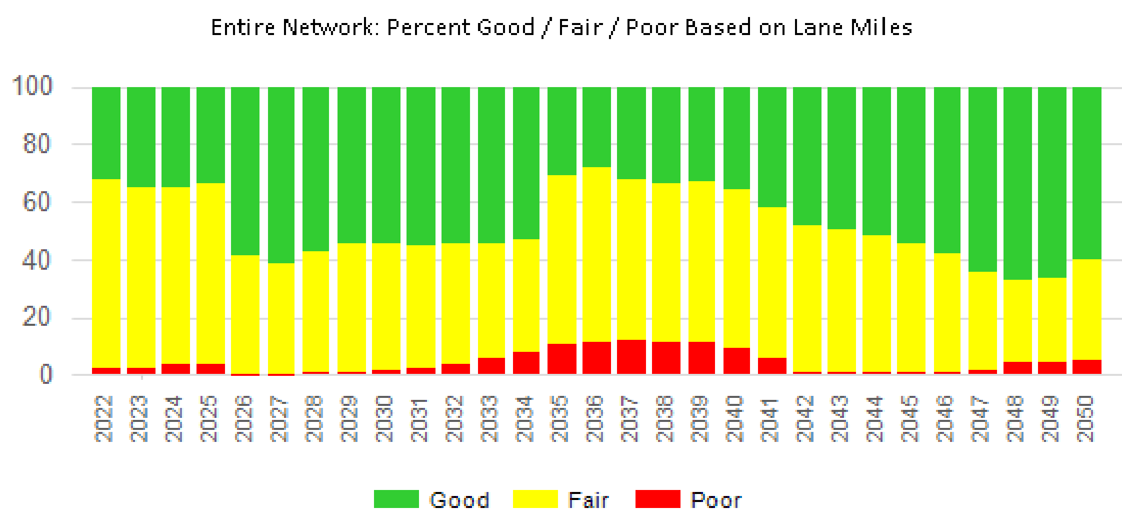

Figure 9: Comparison of condition distribution for the 'Budget 8' scenario

6.4 Dashboards

The results were presented to ADOT in an interactive dashboard that displays data related to the pavement family, sample, regression equations used, and calculated errors. The interactive dashboard was used to discuss and communicate the curve development results. Details on the dashboard are provided below for future reference.

Figure 10 below shows the Family Overview page of the Deterioration Curves Analysis dashboard:

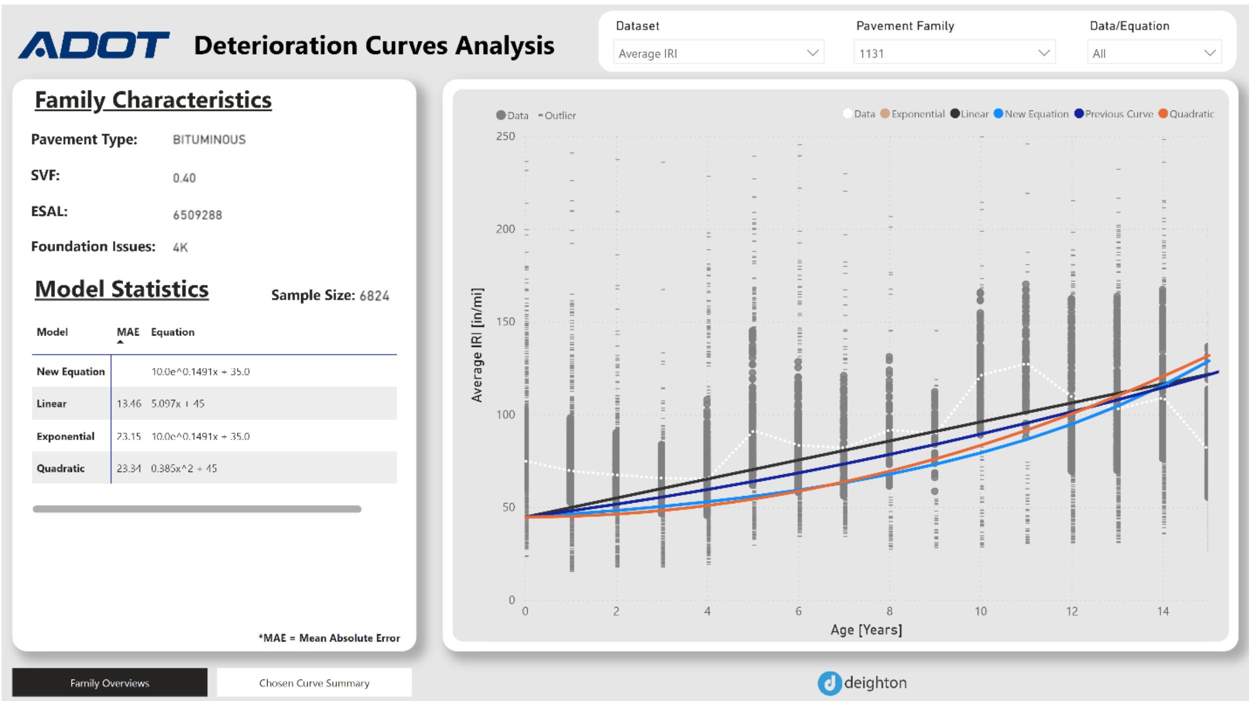

Figure 10: Family Overview page of the Deterioration Curve Analysis dashboard

This page shows the different curve options considered in the curve fitting process one pavement family at a time. It also offers details on the family in the characteristics section. Finally, the Model Statistics section details the performance of each curve and designates the selected curve in the 'New Equation' row.

A new page 'Chosen Curve Summary' was added to the dashboard to give better perspective on the results in the context of the entire condition index, not just the pavement family.

The page is shown in Figure 11 below. It displays the Chosen Curves and the Family Data sections. The Chosen Curves section shows the 15-year projections of the curves generated by Deighton, broken down by pavement family. The Family Data section visualizes the source data provided by ADOT that was ultimately used to generate the curves shown in the Chosen Curve section.

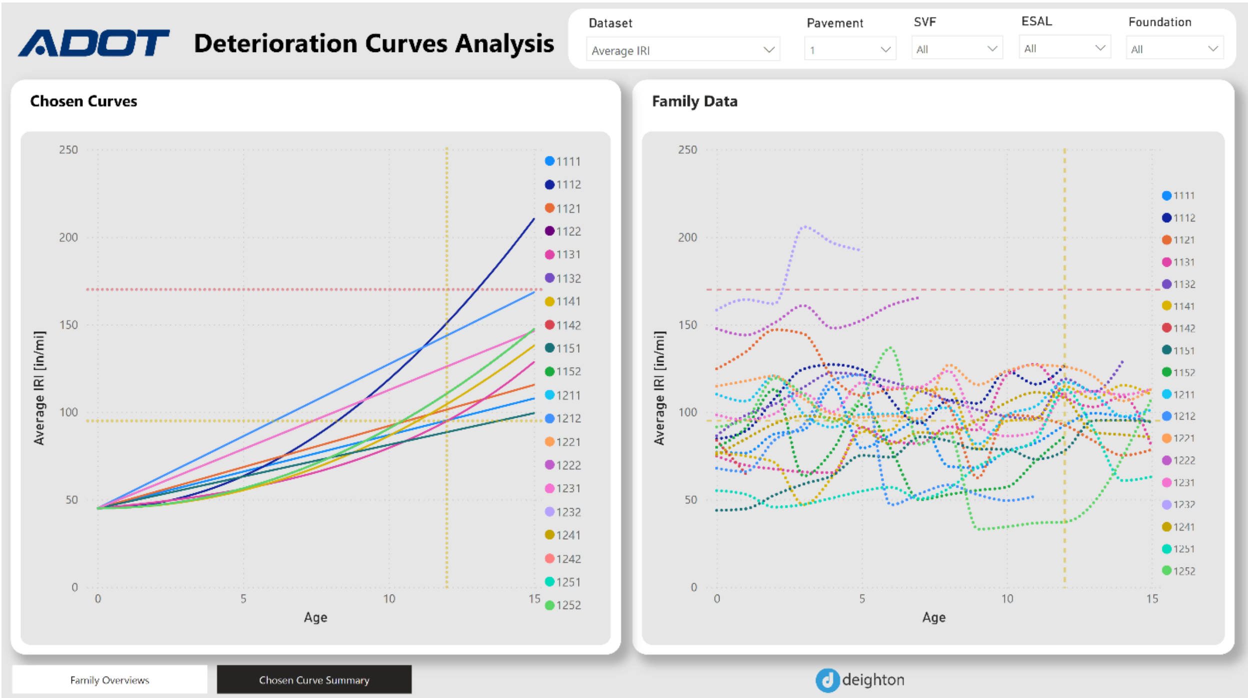

Figure 11 – Chosen Curve Summary page of the Deterioration Curve Analysis dashboard

To access the dashboard, please use the following hyperlink:
[Deterioration Curves Analysis.]

Please contact Deighton Support if you are experiencing issues accessing the dashboard

Appendix A: Analyzing Current Models

In this section, the detailed results from the Analyzing Current Models section can be found. The efficacy of the current models generated were assessed by comparing two consecutive condition points. The first condition was input into the previous model to produce a theoretical condition prediction. This theoretical value was compared with the empirical value found in the following year using scatterplots.

A.1 Avg IRI Current Curve Analysis

Figure 12 below shows the theoretical (forecasted) condition vs the empirical (actual) condition observed in the average IRI data (Empirical-Theoretical series). The 'Empirical' series (y=x) represents the ideal dataset – in this case, where each theoretical prediction perfectly matches the empirical.

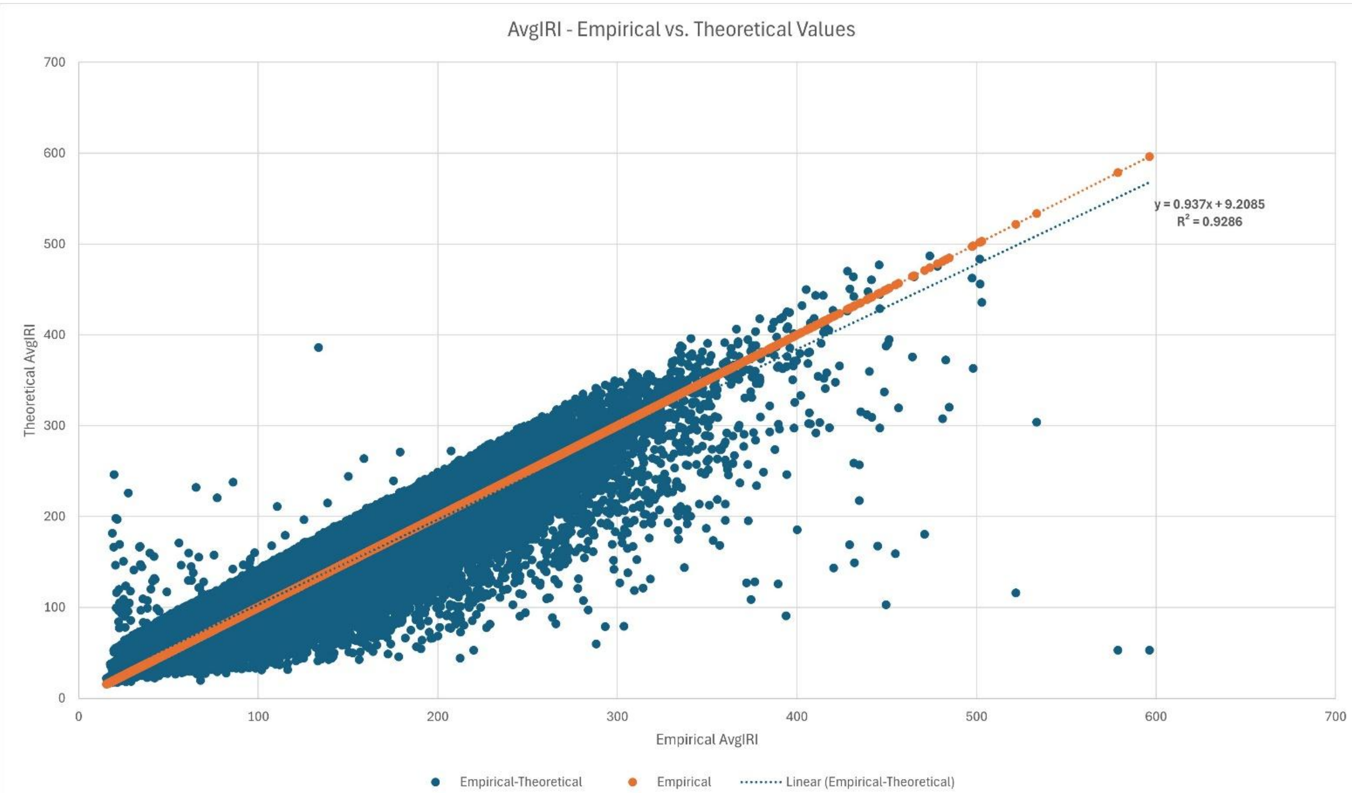

Figure 12 – Avg IRI empirical vs theoretical comparison

This plot was used to analyze the accuracy of the existing condition forecasting models. The linear equation fit to the Empirical-Theoretical dataset is defined as follows:

Equation: Y = 0.937x + 9.2085

Coefficient of determination: R^2 = 0.9286

A.2 Max Rutting Current Curve Analysis

Figure 13 below shows the theoretical (forecasted) condition vs the empirical (actual) condition observed in the max rutting data (Empirical-Theoretical series). The 'Empirical' series (y=x) represents the ideal dataset – in this case, where each theoretical prediction perfectly matches the empirical.

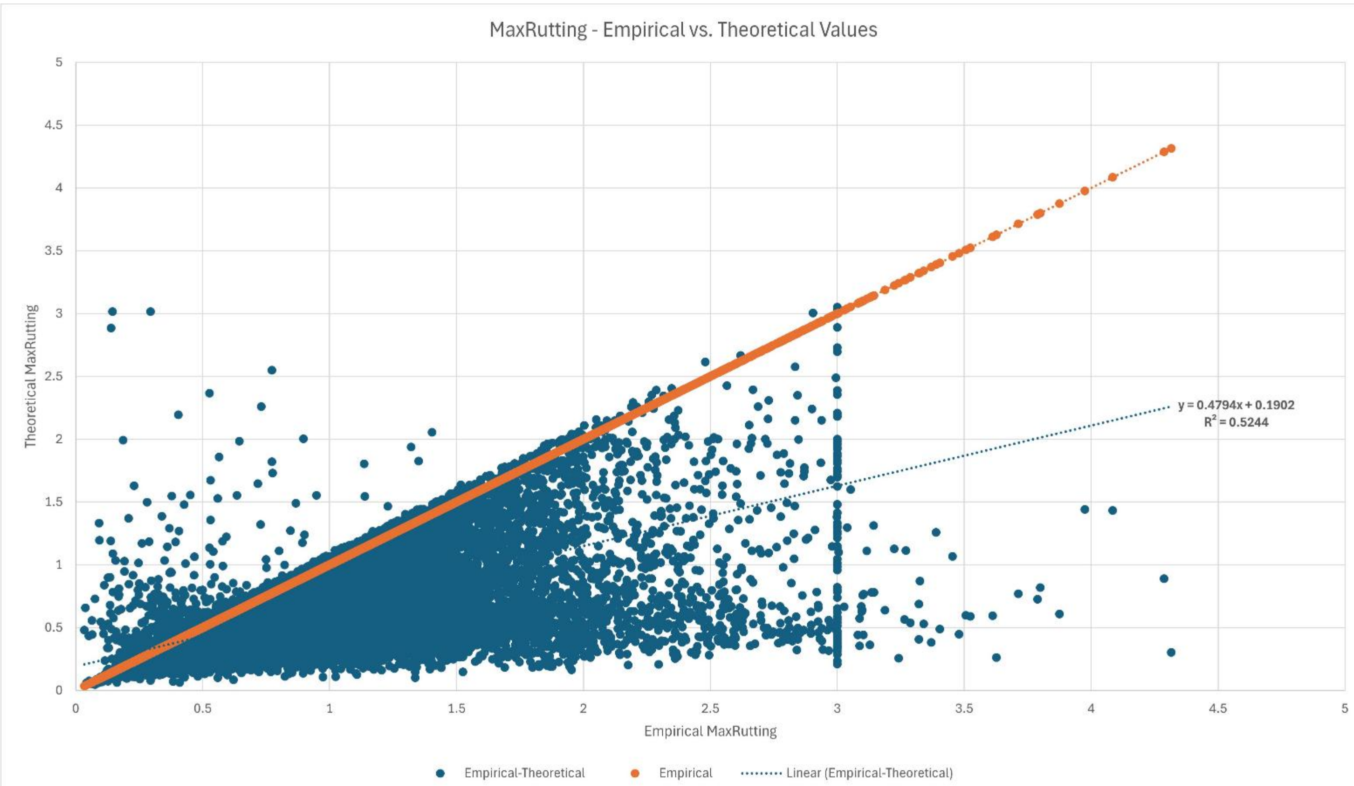

Figure 13 – Max rutting empirical vs theoretical comparison

This plot was used to analyze the accuracy of the existing condition forecasting models. The linear equation fit to the Empirical-Theoretical dataset is defined as follows:

Equation: Y = 0.4794x + 0.1902

Coefficient of determination: R^2 = 0.5244

A.3 Rutting Current Curve Analysis

Figure 14 below shows the theoretical (forecasted) condition vs the empirical (actual) condition observed in the rutting data (Empirical-Theoretical series). The 'Empirical' series (y=x) represents the ideal dataset – in this case, where each theoretical prediction perfectly matches the empirical.

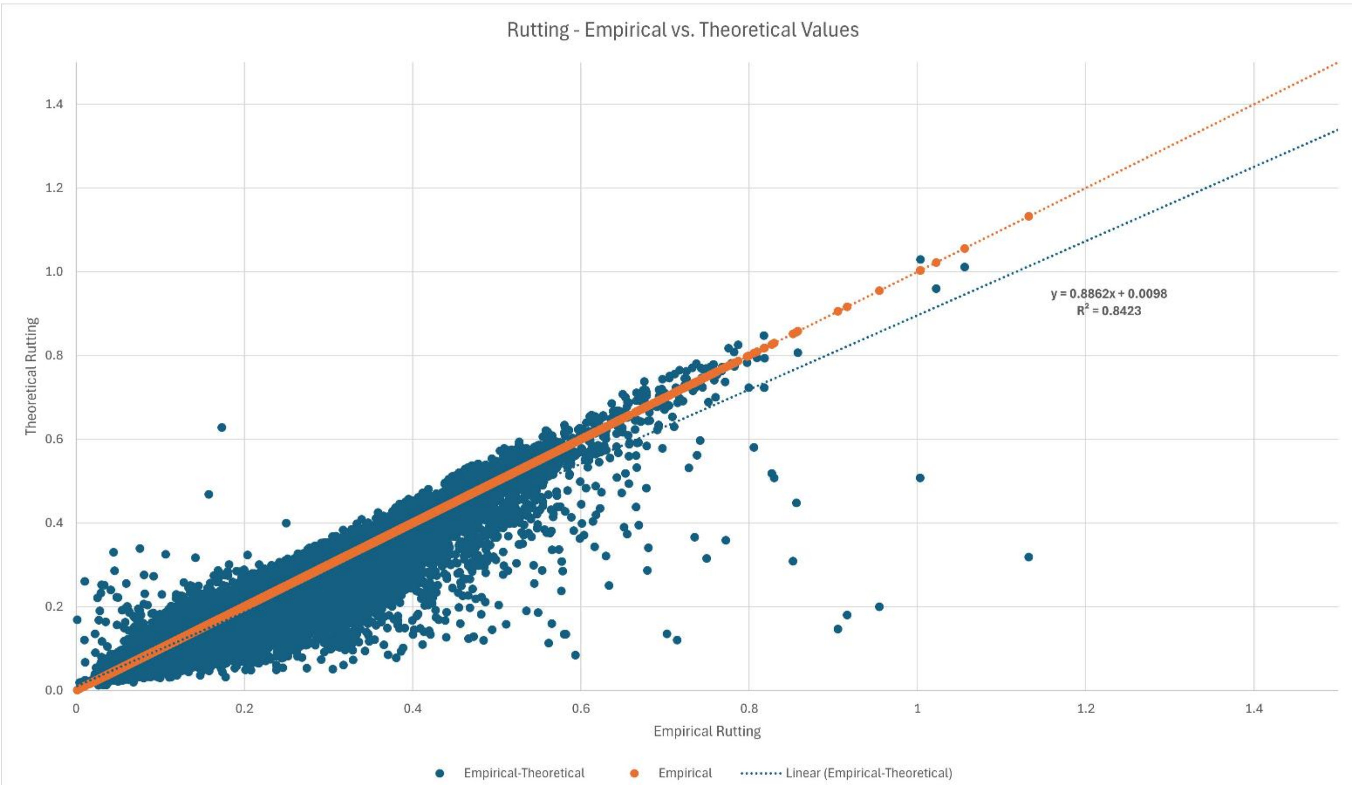

Figure 14 – Rutting empirical vs theoretical comparison

This plot was used to analyze the accuracy of the existing condition forecasting models. The linear equation fit to the Empirical-Theoretical dataset is defined as follows:

Equation: Y = 0.8862x + 0.00982

Coefficient of determination: $R^2 = 0.8423$

A.4 HPMS Cracking Current Curve Analysis

Figure 15 below shows the theoretical (forecasted) condition vs the empirical (actual) condition observed in the HPMS cracking data (Empirical-Theoretical series). The 'Empirical' series (y=x) represents the ideal dataset – in this case, where each theoretical prediction perfectly matches the empirical.

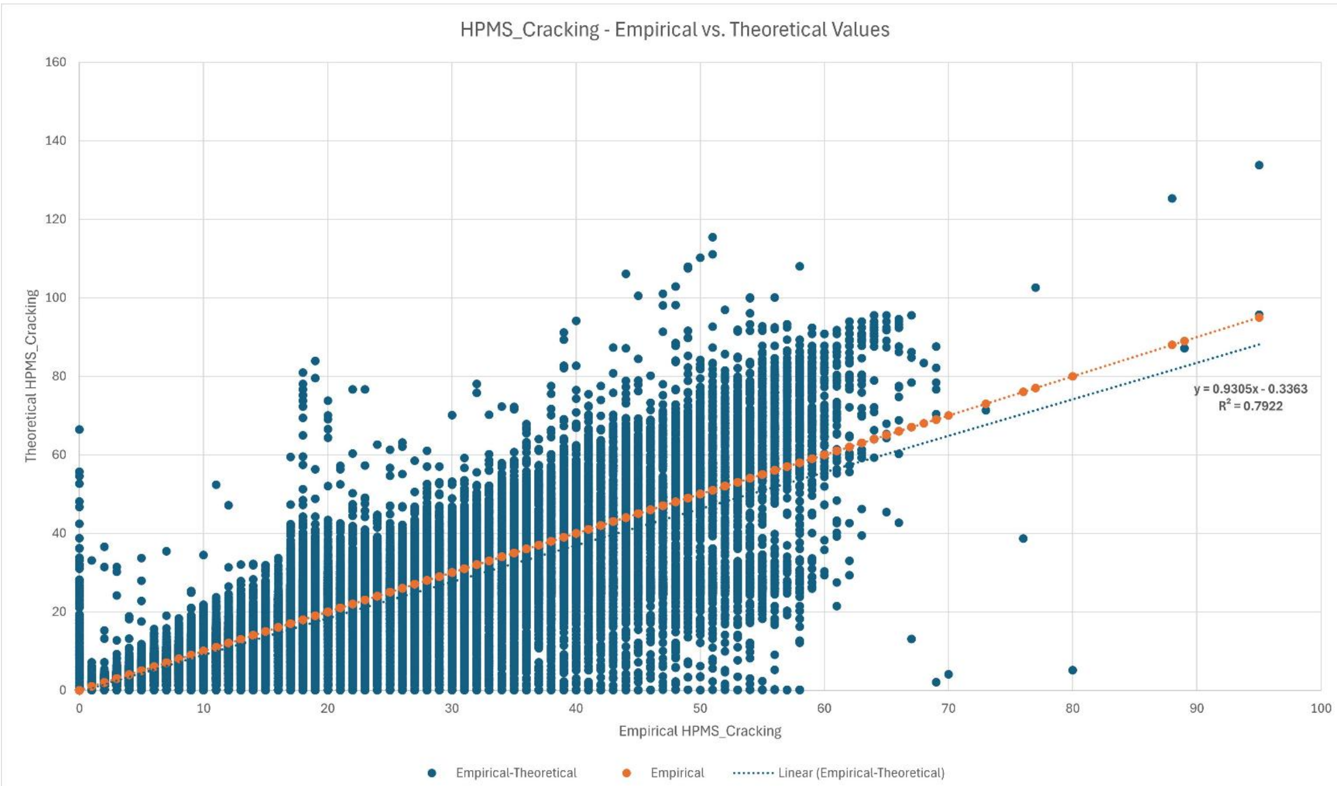

Figure 15 – HPMS cracking empirical vs theoretical comparison

This plot was used to analyze the accuracy of the existing condition forecasting models. The linear equation fit to the Empirical-Theoretical dataset is defined as follows:

Equation: Y = 0.9305x + 0.9305

Coefficient of determination: R^2 = 0.7922

A.5 Cracking Percent Current Curve Analysis

Figure 16 below shows the theoretical (forecasted) condition vs the empirical (actual) condition observed in the cracking percent data (Empirical-Theoretical series). The 'Empirical' series (y=x) represents the ideal dataset – in this case, where each theoretical prediction perfectly matches the empirical.

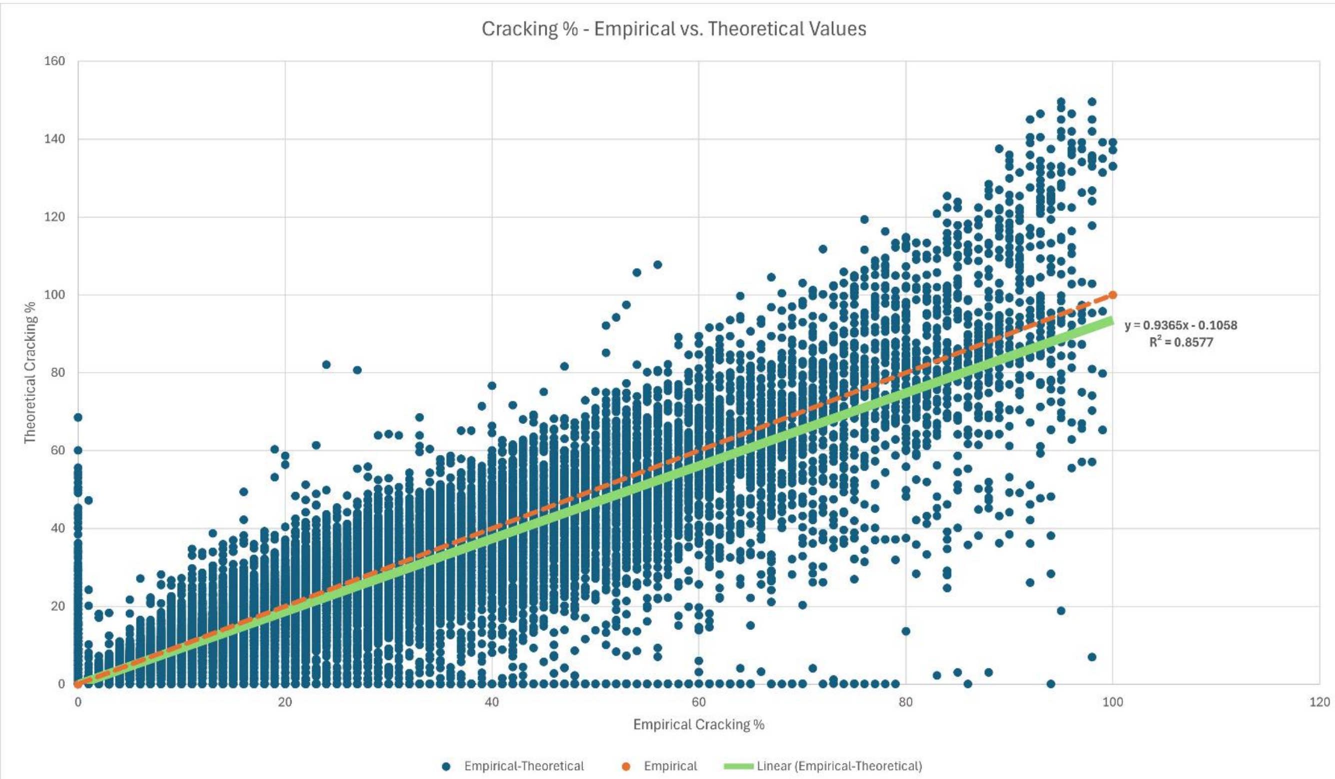

Figure 16 –Cracking percent empirical vs theoretical comparison

This plot was used to analyze the accuracy of the existing condition forecasting models. The linear equation fit to the Empirical-Theoretical dataset is defined as follows:

Equation: Y = 0.9365x + 0.1058

Coefficient of determination: R^2 = 0.8577

A.6 Max Faulting Current Curve Analysis

Figure 17 below shows the theoretical (forecasted) condition vs the empirical (actual) condition observed in the max faulting data (Empirical-Theoretical series). The ‘Empirical’ series (y=x) represents the ideal dataset – in this case, where each theoretical prediction perfectly matches the empirical.

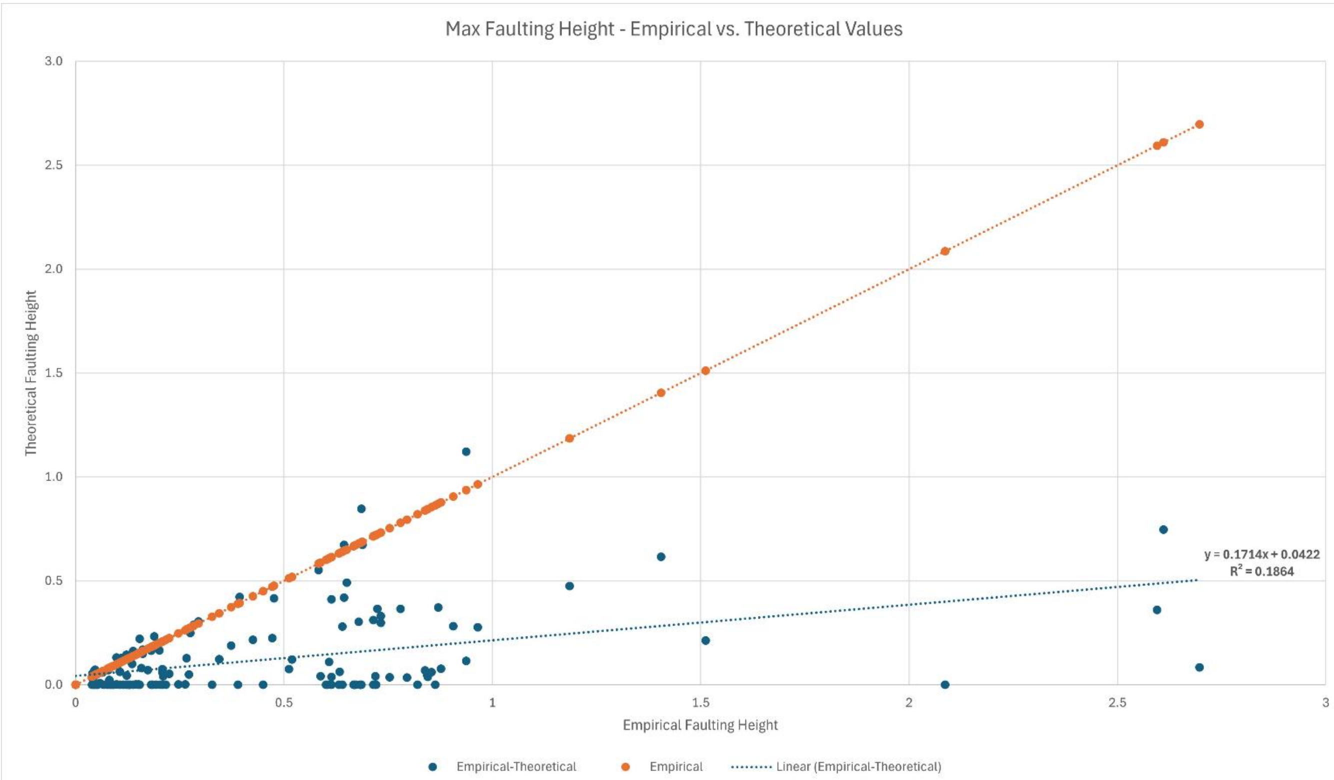

Figure 17 –Max faulting percent empirical vs theoretical comparison

This plot was used to analyze the accuracy of the existing condition forecasting models. The linear equation fit to the Empirical-Theoretical dataset is defined as follows:

Equation: Y = 0.1714x + 0.0422

Coefficient of determination: $R^2 = 0.1864$

A.7 Mean Faulting Current Curve Analysis

Figure 18 below shows the theoretical (forecasted) condition vs the empirical (actual) condition observed in the mean faulting data (Empirical-Theoretical series). The 'Empirical' series (y=x) represents the ideal dataset – in this case, where each theoretical prediction perfectly matches the empirical.

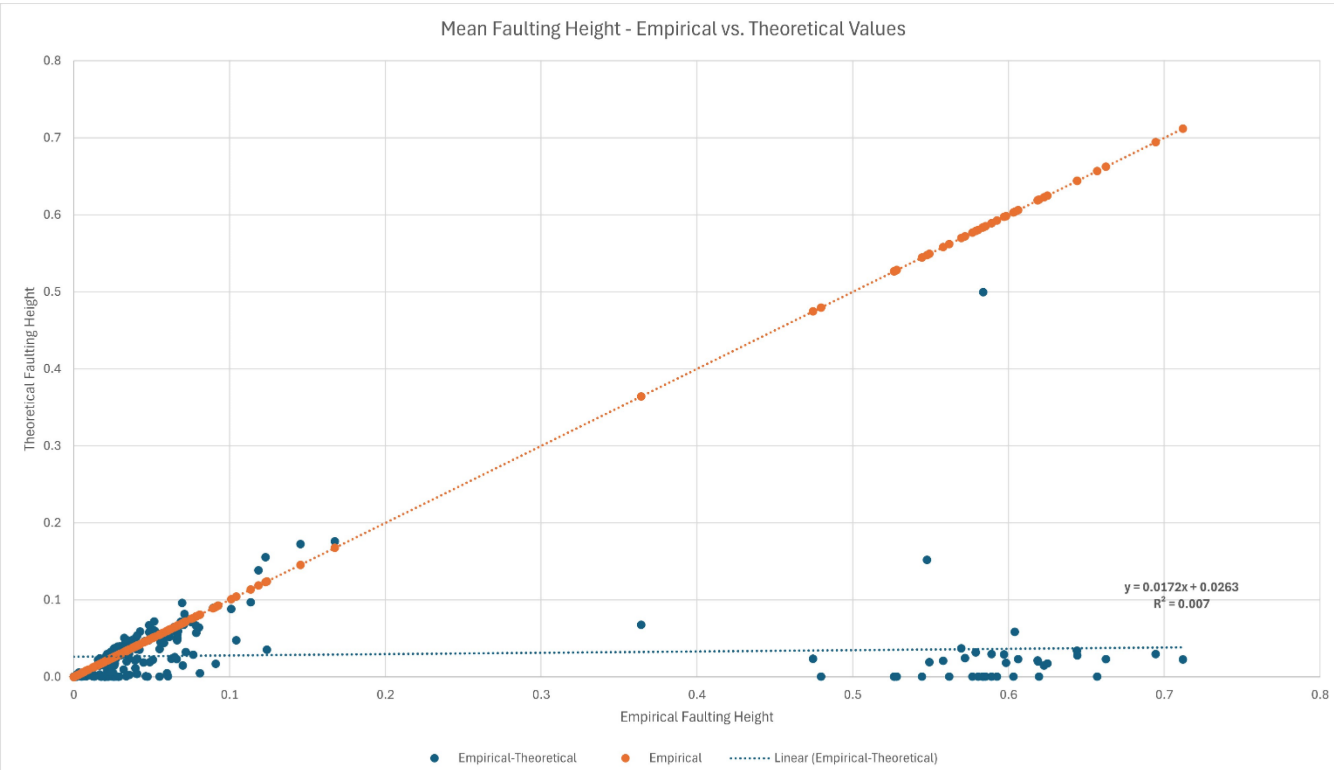

Figure 18 –Mean faulting percent empirical vs theoretical comparison

This plot was used to analyze the accuracy of the existing condition forecasting models. The linear equation fit to the Empirical-Theoretical dataset is defined as follows:

Equation: Y = 0.0172x + 0.0263

Coefficient of determination: R^2 = 0.007

Appendix B: Analyzing Family of Curves

This section demonstrates the results of the procedure outlined in the Analyzing Curve Families section. Each condition variable is broken down into the codes associated with each family category:

- Pavement Type
- Seasonal Variation Factor (SVF)
- Equivalent Single Axial Loads (ESAL)
- Foundation Issues

Section 2.4 details the different codes in each category and how they were determined. For each of these codes, the observed year-to-year increases in deterioration were profiled into different categories. The categories used for each of the condition variables are listed in Table 12 below.

Condition Variables	Deterioration Change Categories	Change Unit
Rutting (inch) **Max Rutting** (inch)	0-0.025 0.025-0.050 0.050-0.075 0.075-0.1 0.1+	Inch
Mean Faulting Height (inch) **Max Faulting Height** (inch)	0-0.1 0.1-0.2 0.2-0.3 0.3+	Inch
Avg IRI (inch/mi) **HPMS Cracking** (% wheel path) **Cracking Percent** (% whole lane)	0-5 5-10 10-15 15-20 20+	Refer to condition variable for unit

Table 17: Deterioration categories used for each condition variable

The data here was used to assess the statistical significance of the family codes used in this pavement analysis; the behavior of each code varies enough for Deighton to conclude their existence is a benefit to ADOT and deterioration modelling.

B.1 Avg IRI: Pavement Type

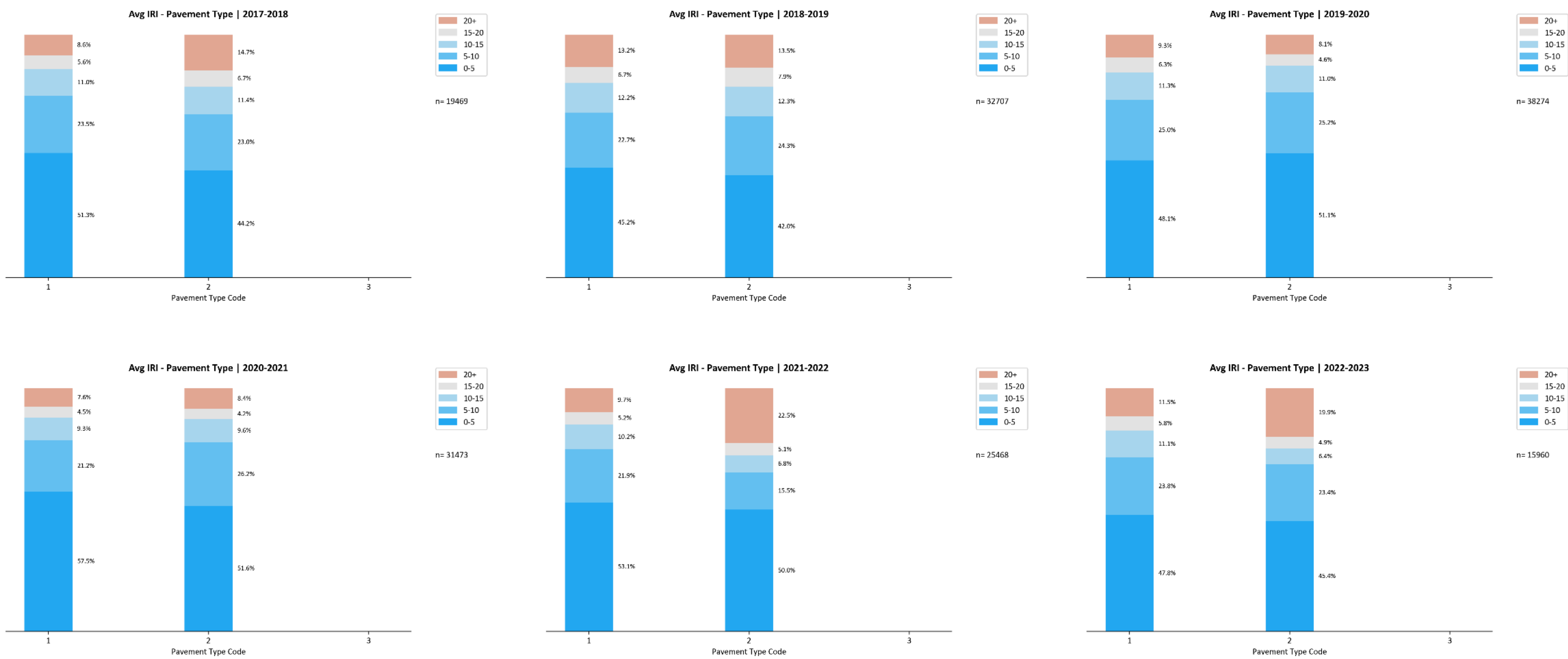

Figure 19 – Year-to-year average IRI deterioration range distributions based on pavement type

B.2 Avg IRI: SVF

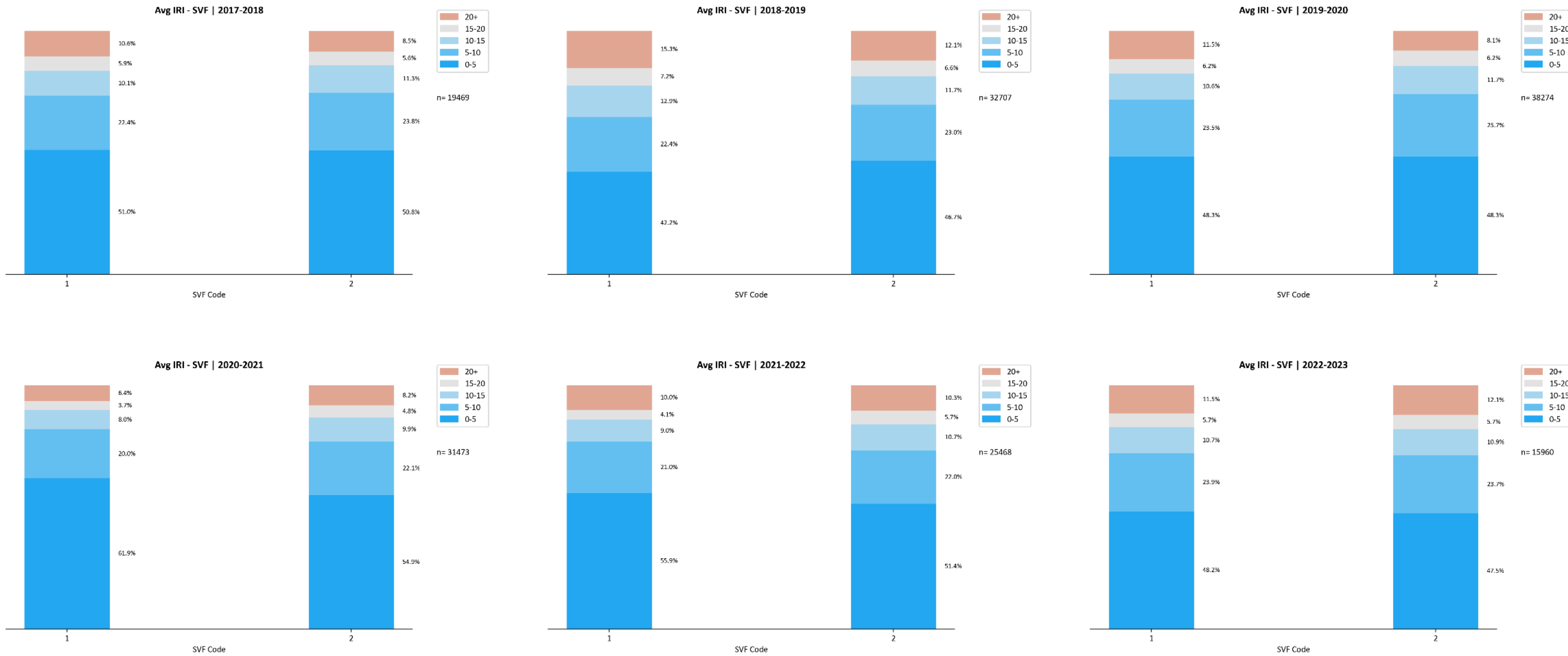

Figure 20 - Year-to-year average IRI deterioration range distributions based on seasonal variation factor (SVF)

B.3 Avg IRI: ESAL

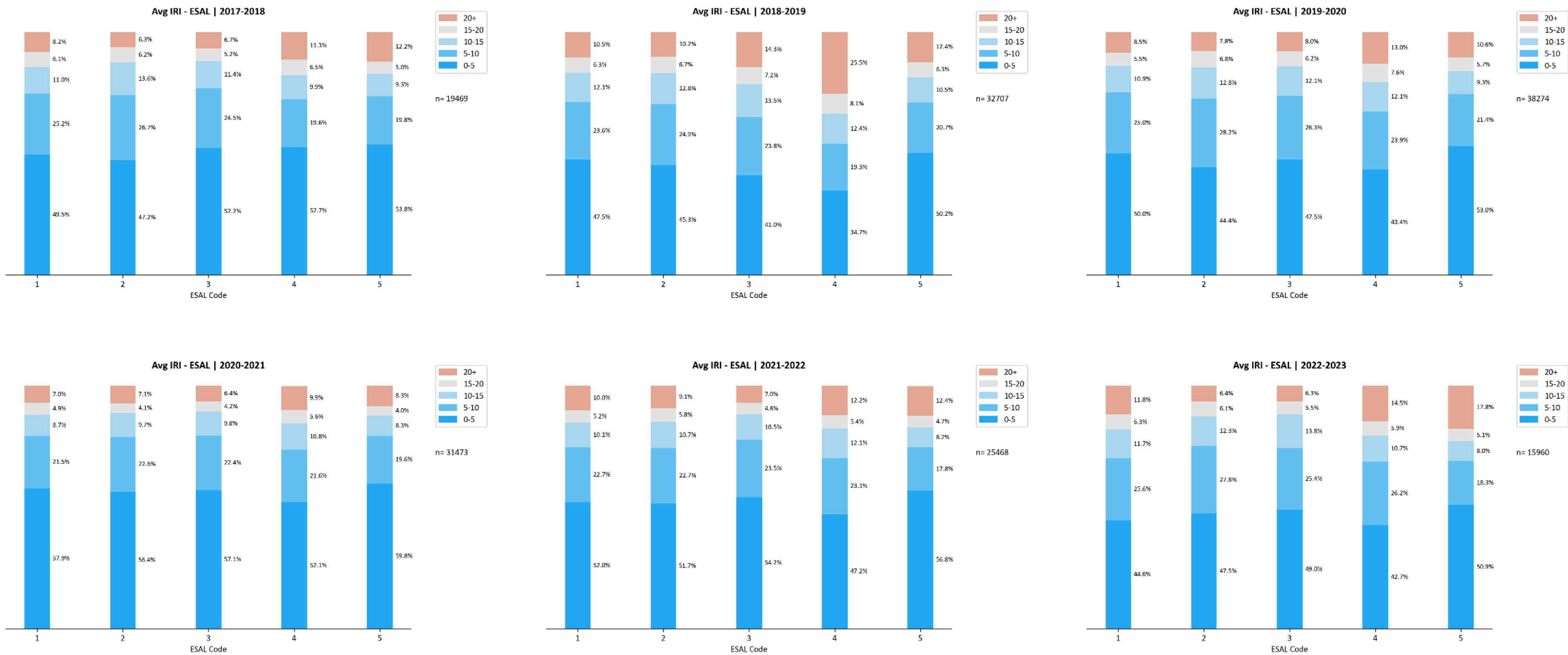

Figure 21 - Year-to-year average IRI deterioration range distributions based on equivalent single axial load (ESAL)

B.4 Avg IRI: Foundation

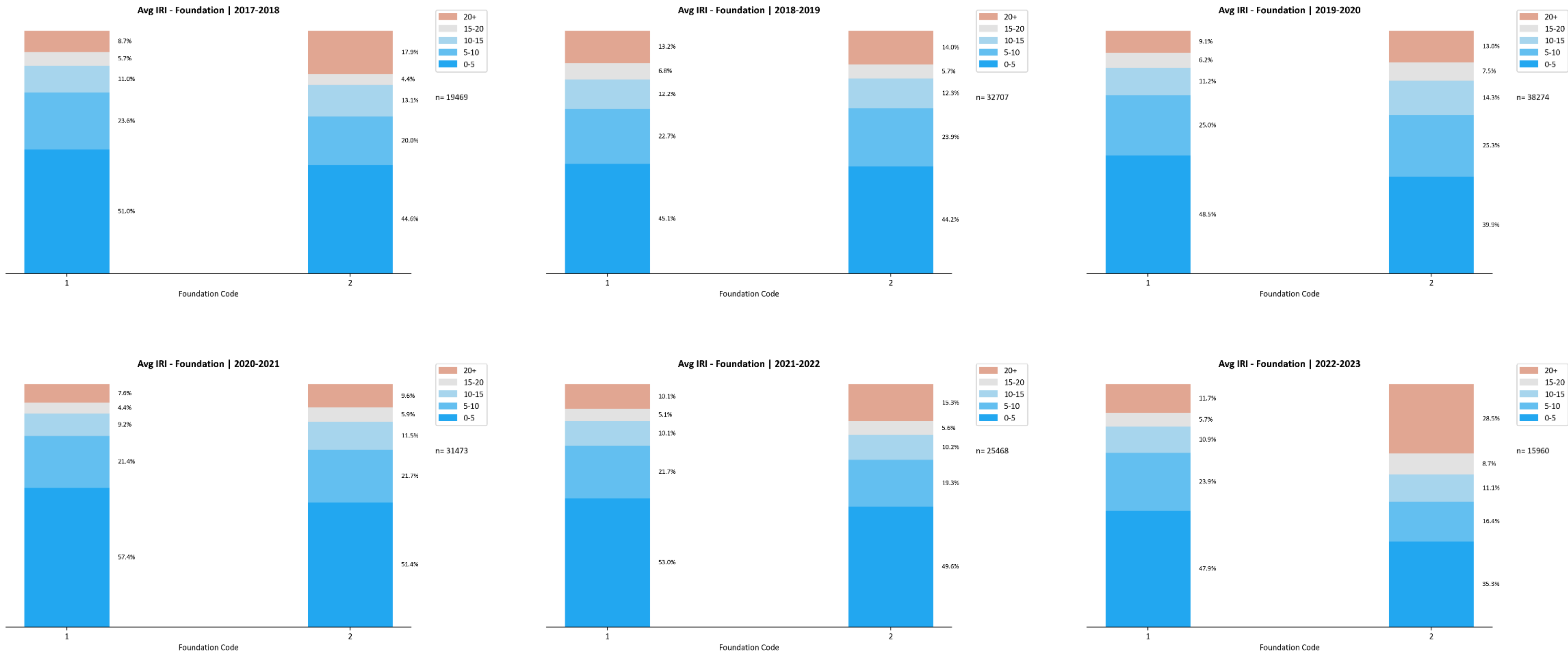

Figure 22 - Year-to-year average IRI deterioration range distributions based on foundation issues

B.5 Max Rutting: Pavement Type

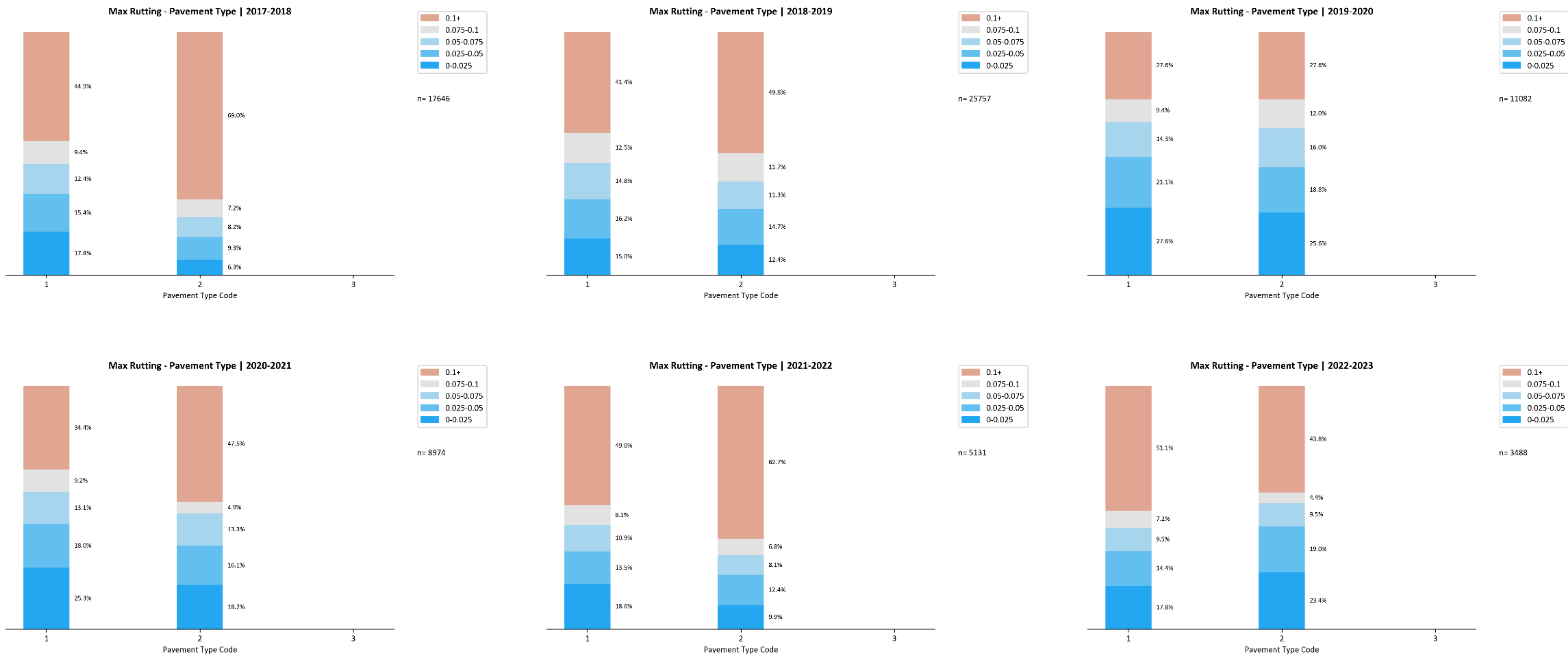

Figure 23 - Year-to-year max rutting deterioration range distributions based on pavement type

B.6 Max Rutting: SVF

B.7

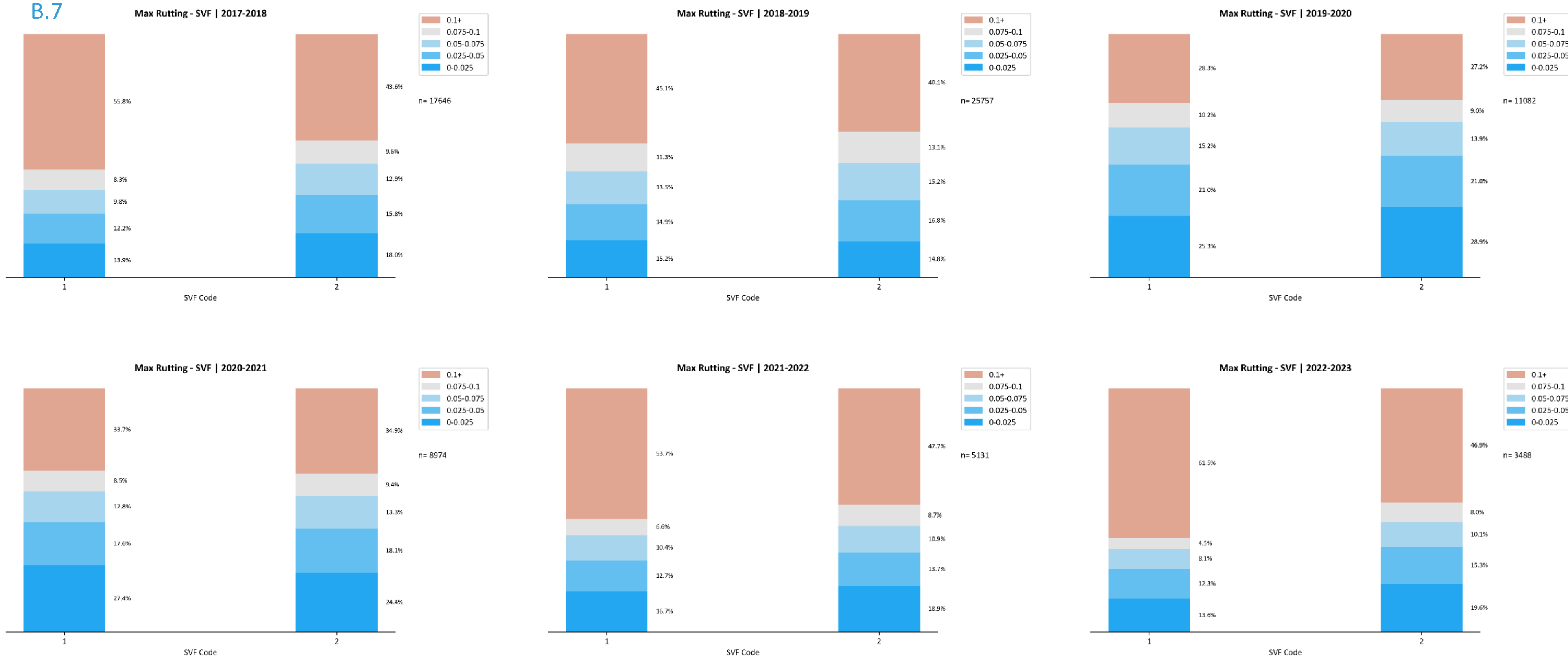

Figure 24 - Year-to-year max rutting deterioration range distributions based on seasonal variation factor (SVF)

B.8 Max Rutting: ESAL

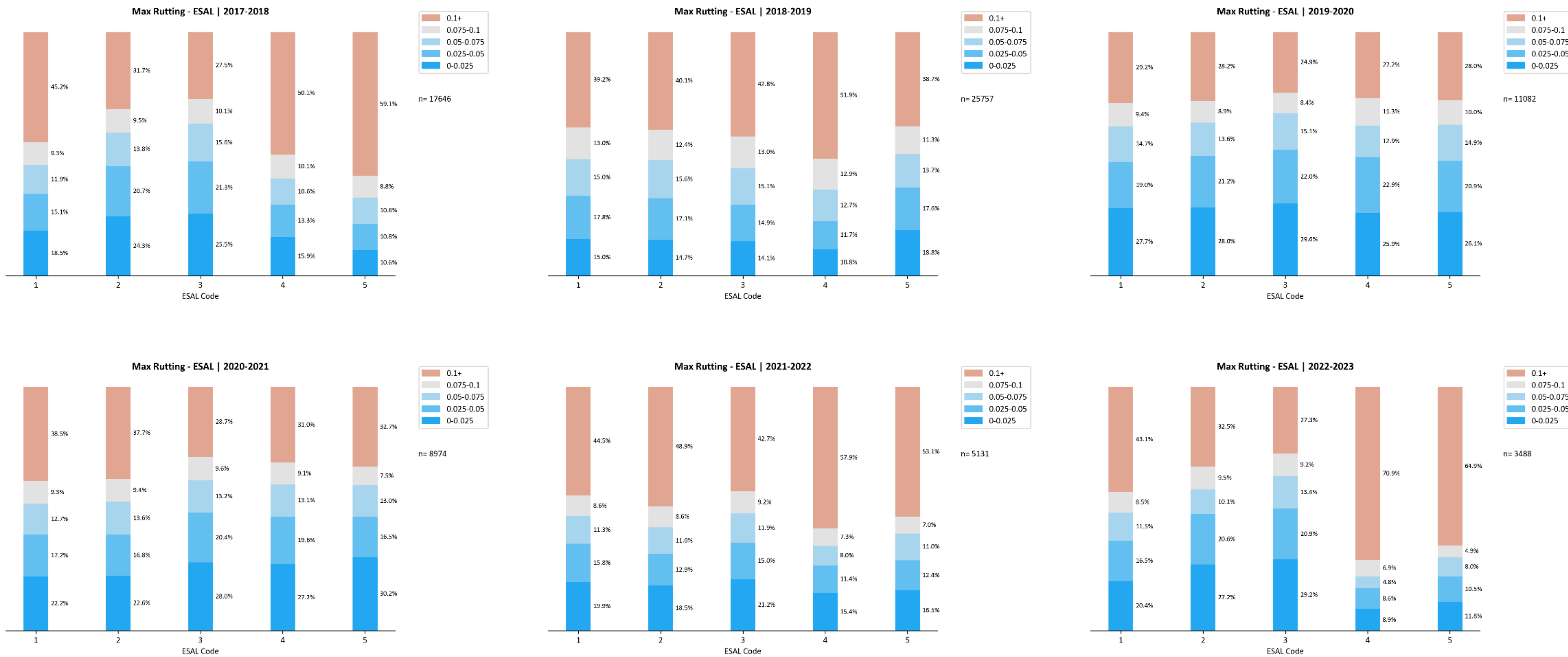

Figure 25 - Year-to-year max rutting deterioration range distributions based on equivalent single axial load (ESAL)

B.9 Max Rutting: Foundation

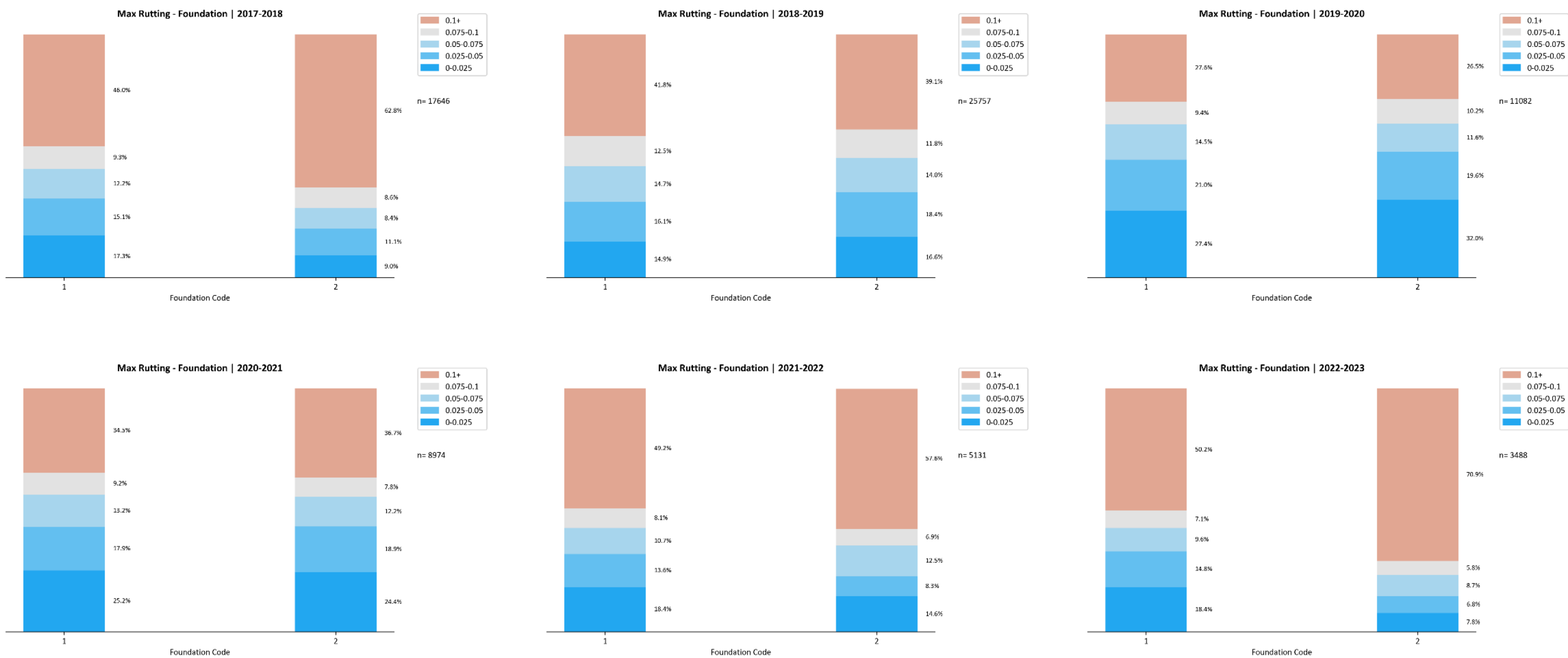

Figure 26 - Year-to-year max rutting deterioration range distributions based on foundation issues

B.10 Rutting: Pavement Type

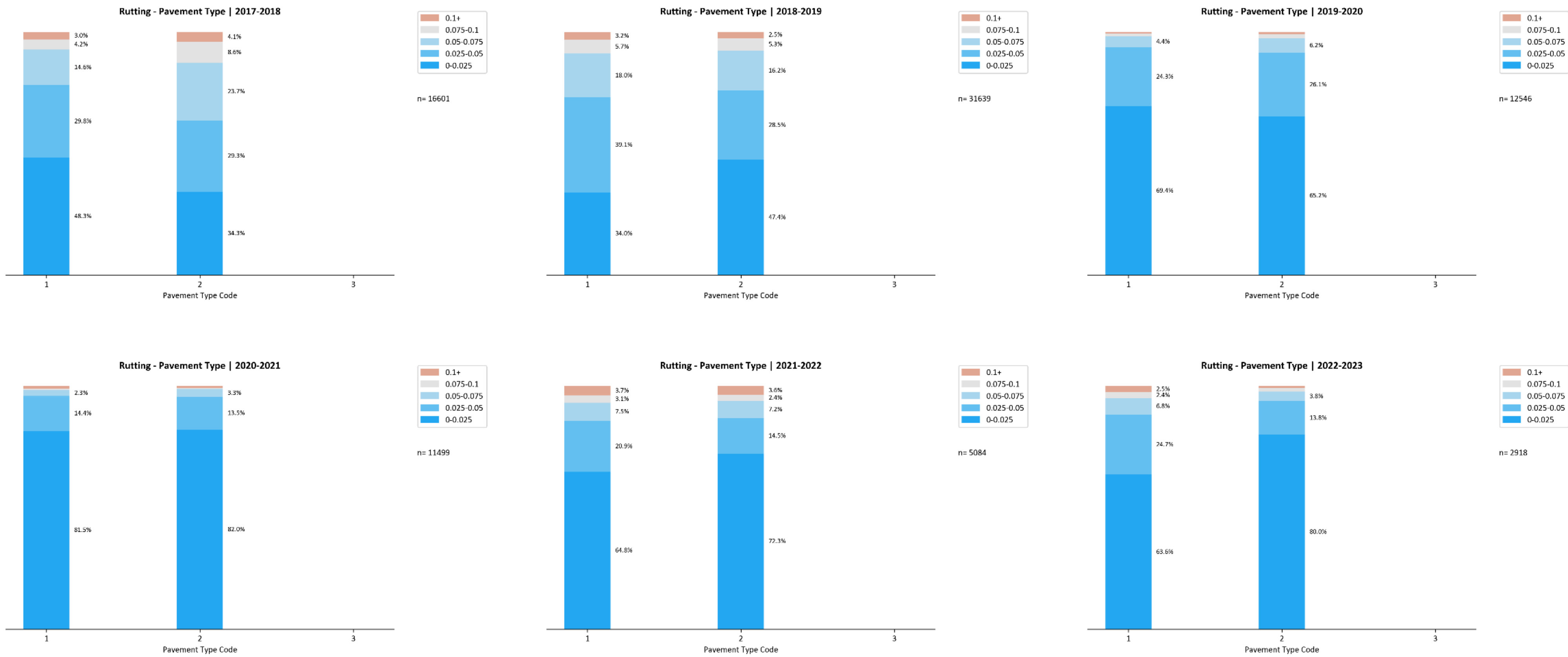

Figure 27 - Year-to-year rutting deterioration range distributions based on pavement type

B.11 Rutting: SVF

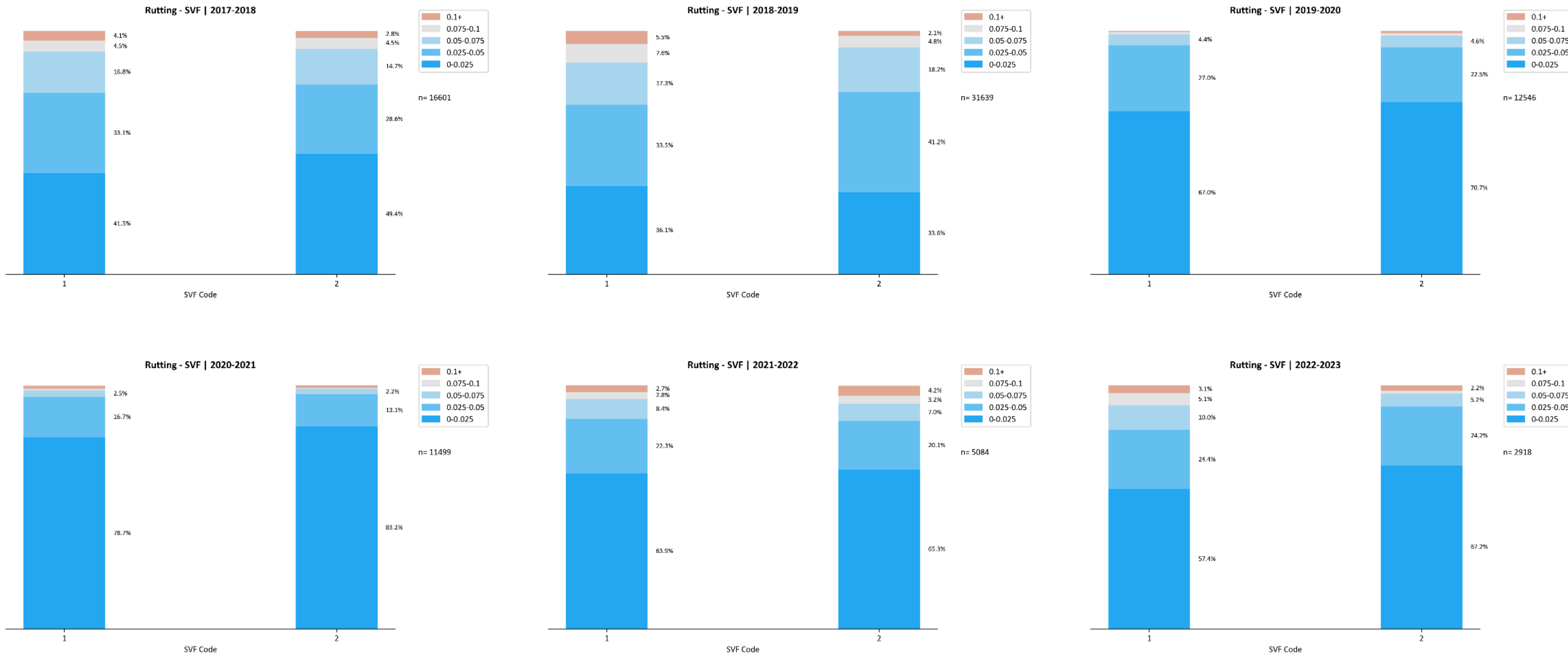

Figure 28 - Year-to-year rutting deterioration range distributions based on seasonal variation factor (SVF)

B.12 Rutting: ESAL

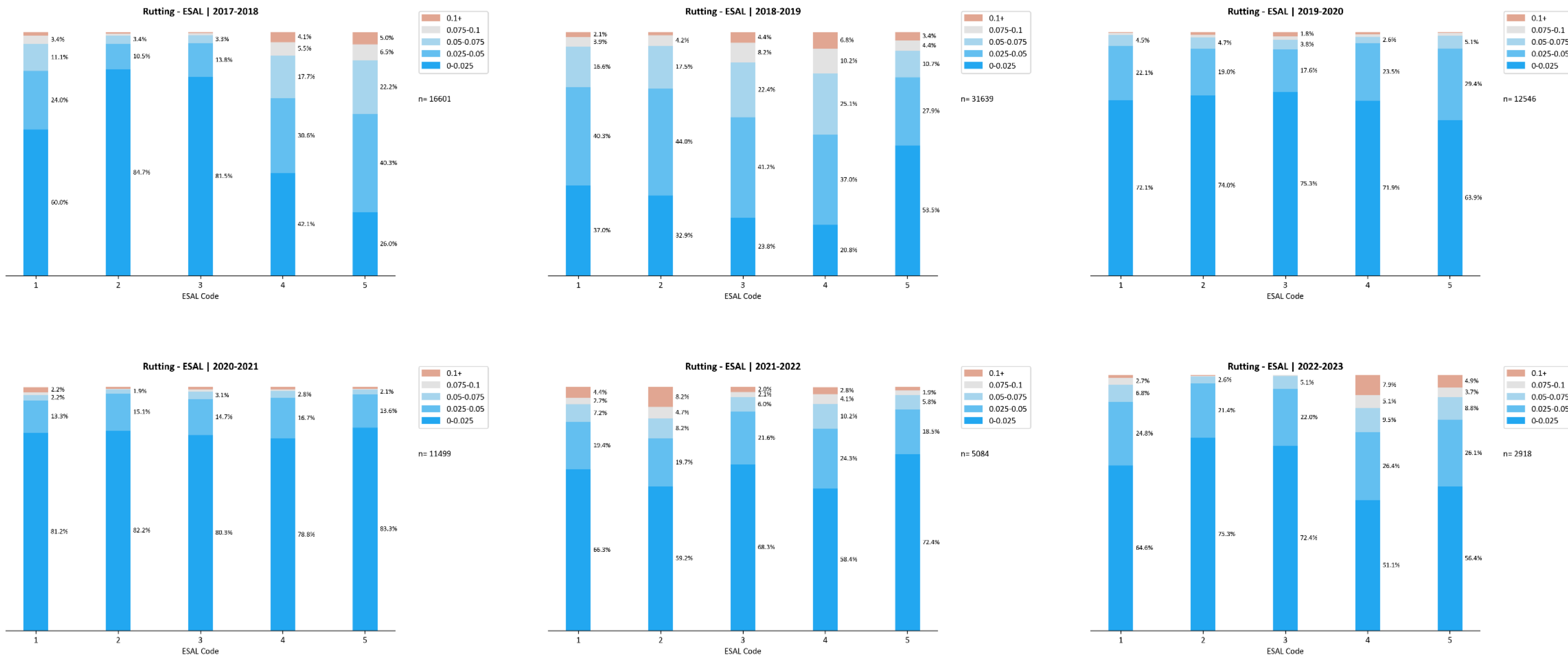

Figure 29 - Year-to-year rutting deterioration range distributions based on equivalent single axial load (ESAL)

B.13 Rutting: Foundation

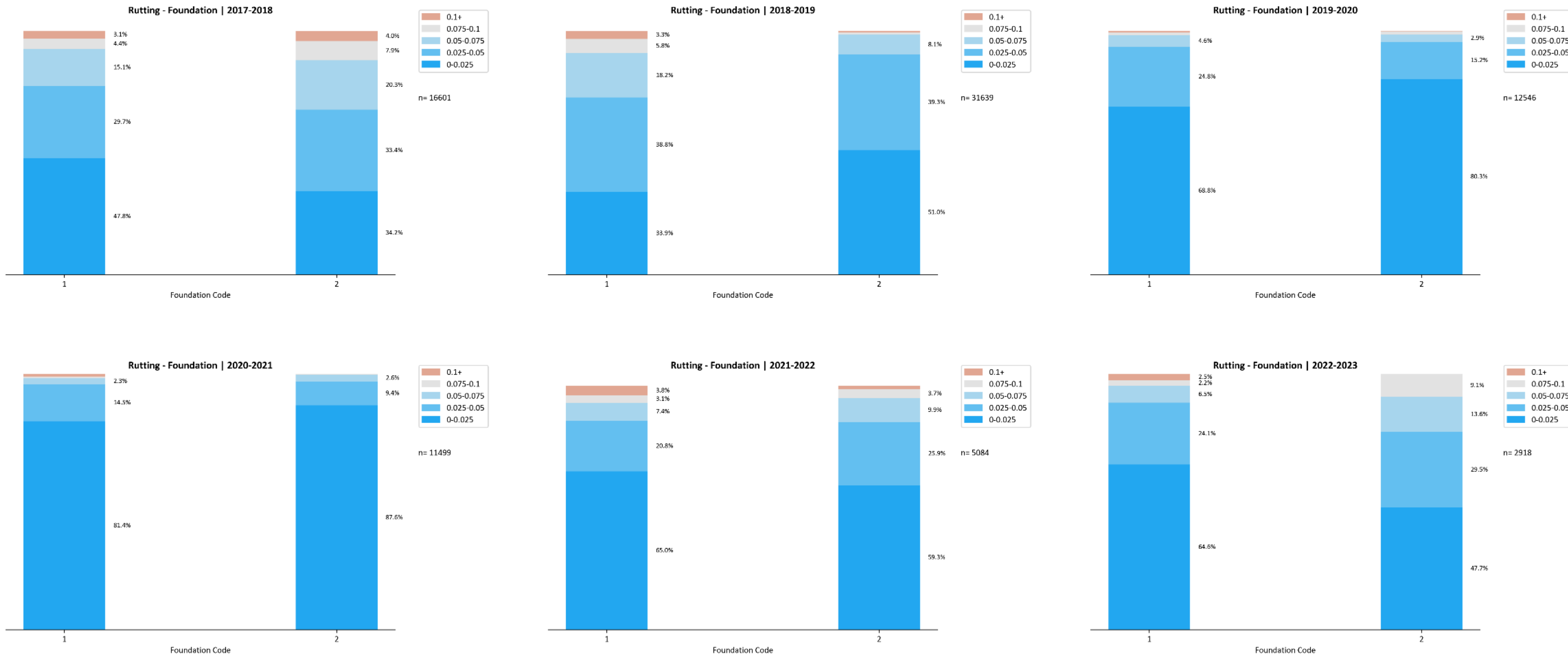

Figure 30 - Year-to-year rutting deterioration range distributions based on foundation issues

B.14 HPMS Cracking: Pavement Type

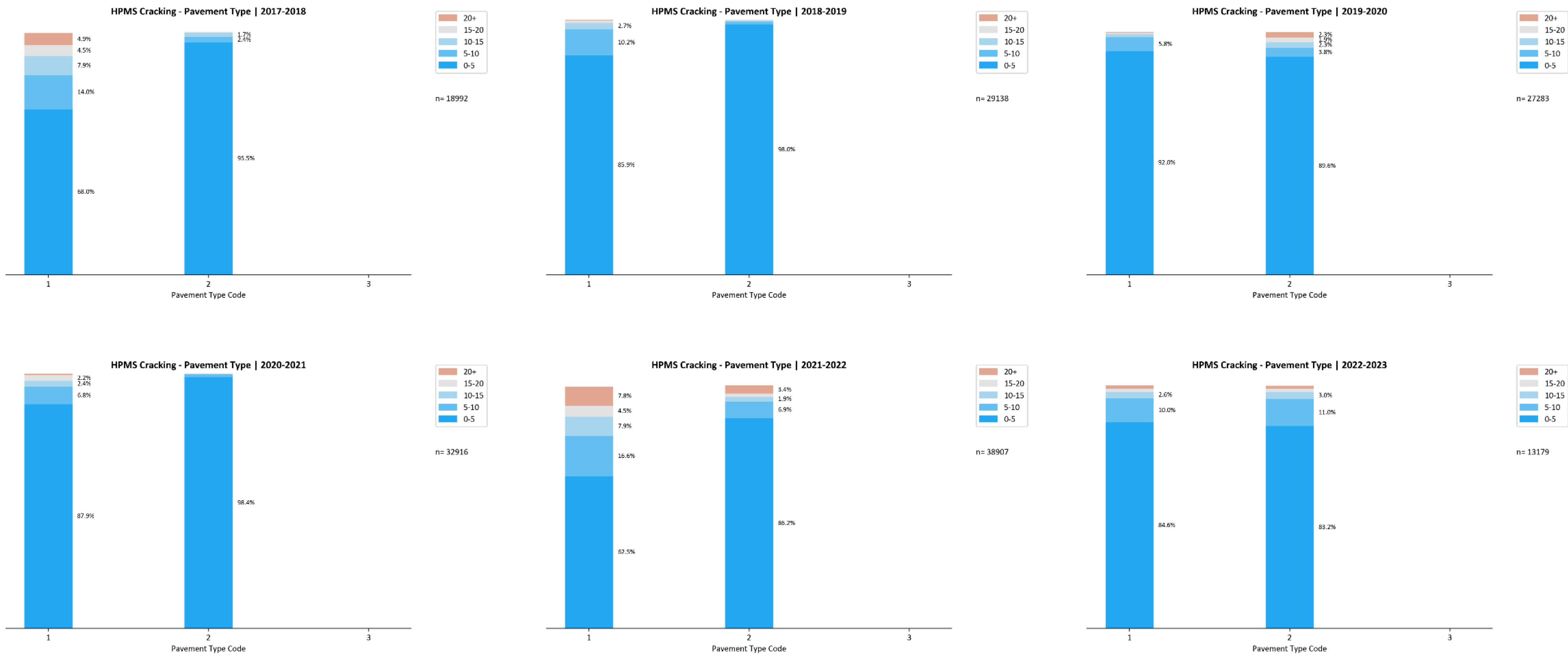

Figure 31 -Year-to-year HPMS cracking deterioration range distributions based on foundation issues

B.15 HPMS Cracking: SVF

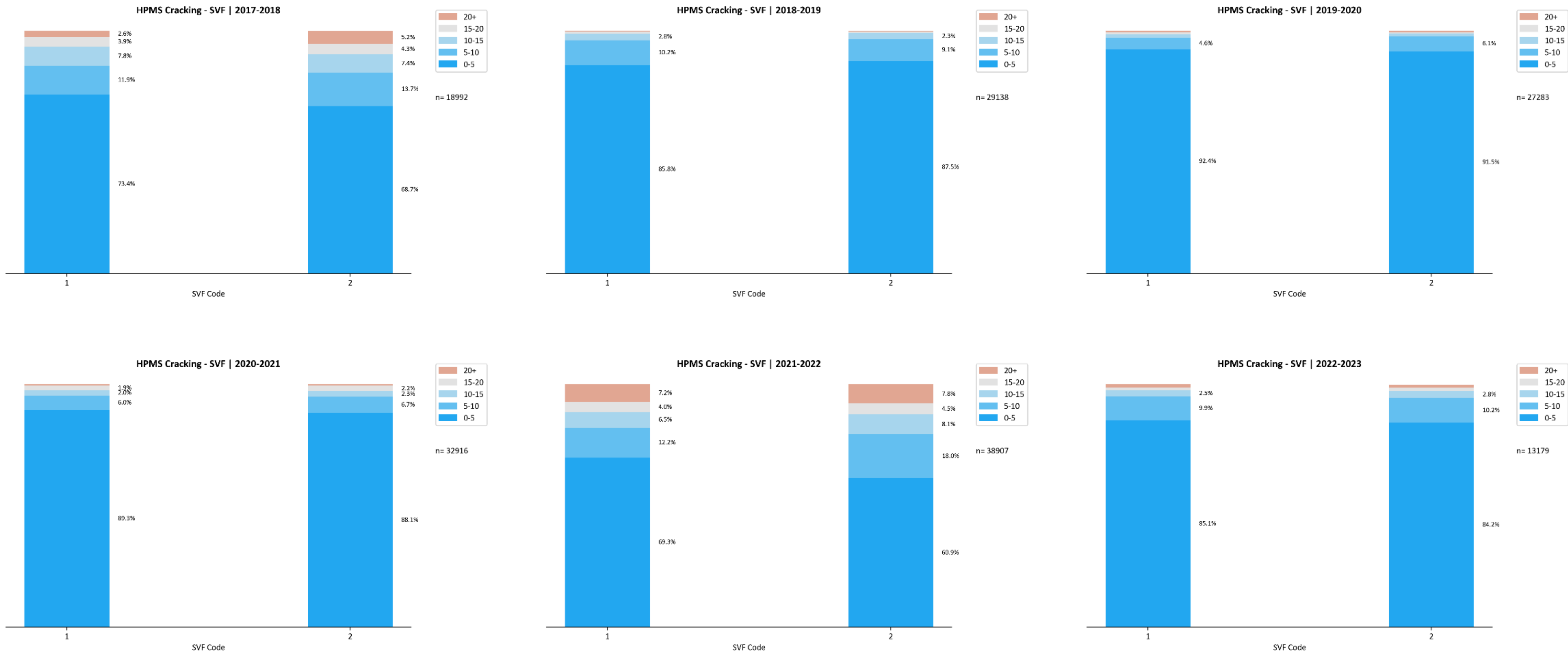

Figure 32 - Year-to-year HPMS cracking deterioration range distributions based on seasonal variation factor (SVF)

B.16 HPMS Cracking: ESAL

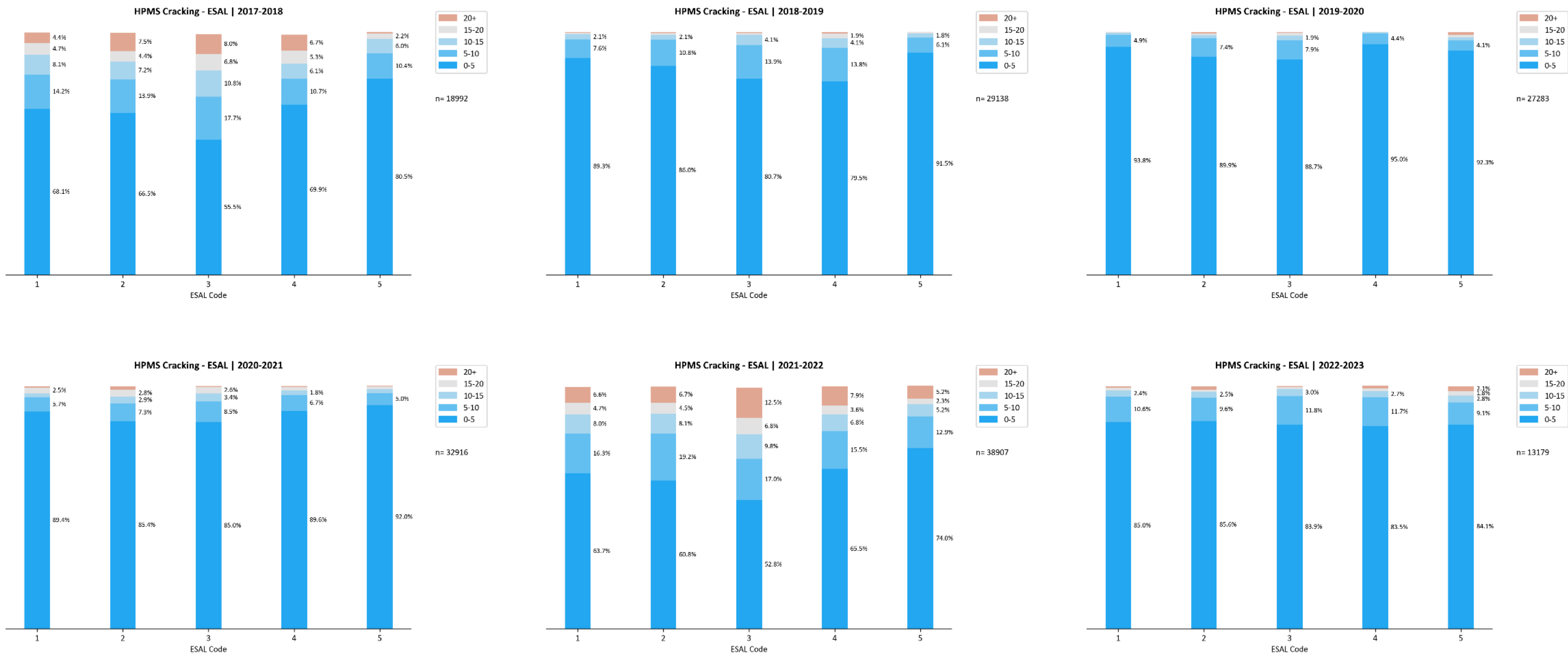

Figure 33 - Year-to-year HPMS cracking deterioration range distributions based on equivalent single axial load (ESAL)

B.17 HPMS Cracking: Foundation

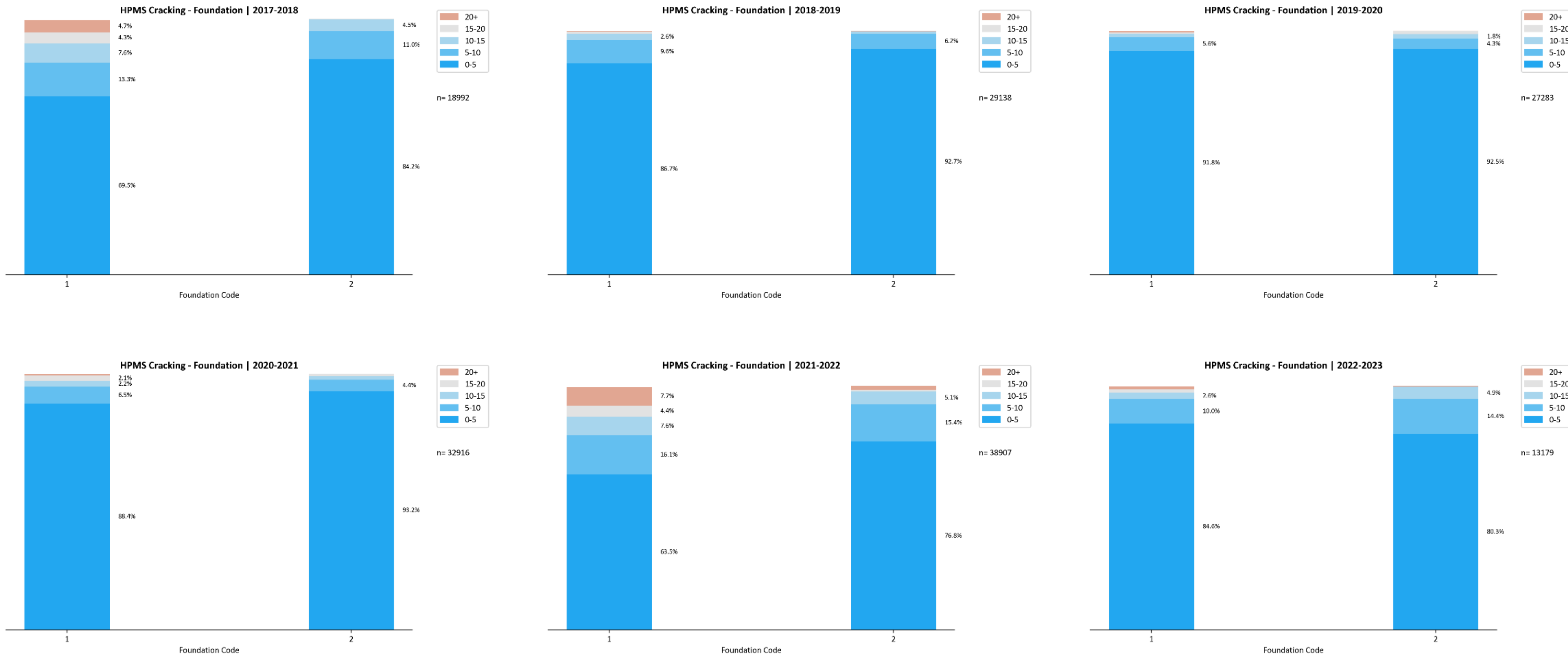

Figure 34 - Year-to-year HPMS cracking deterioration range distributions based on foundation issues

B.18 Cracking Percent: Pavement Type

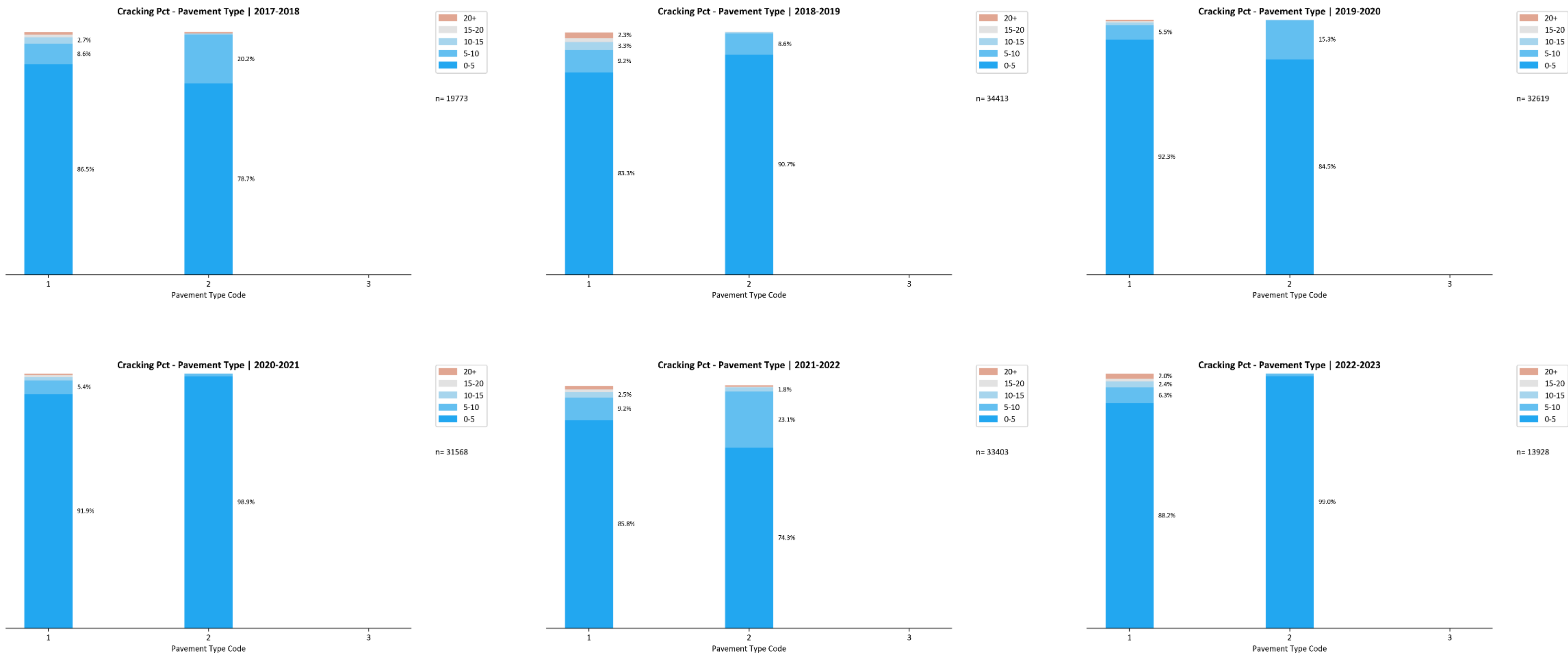

Figure 35 -Year-to-year cracking percent deterioration range distributions based on pavement type

B.19 Cracking Percent: SVF

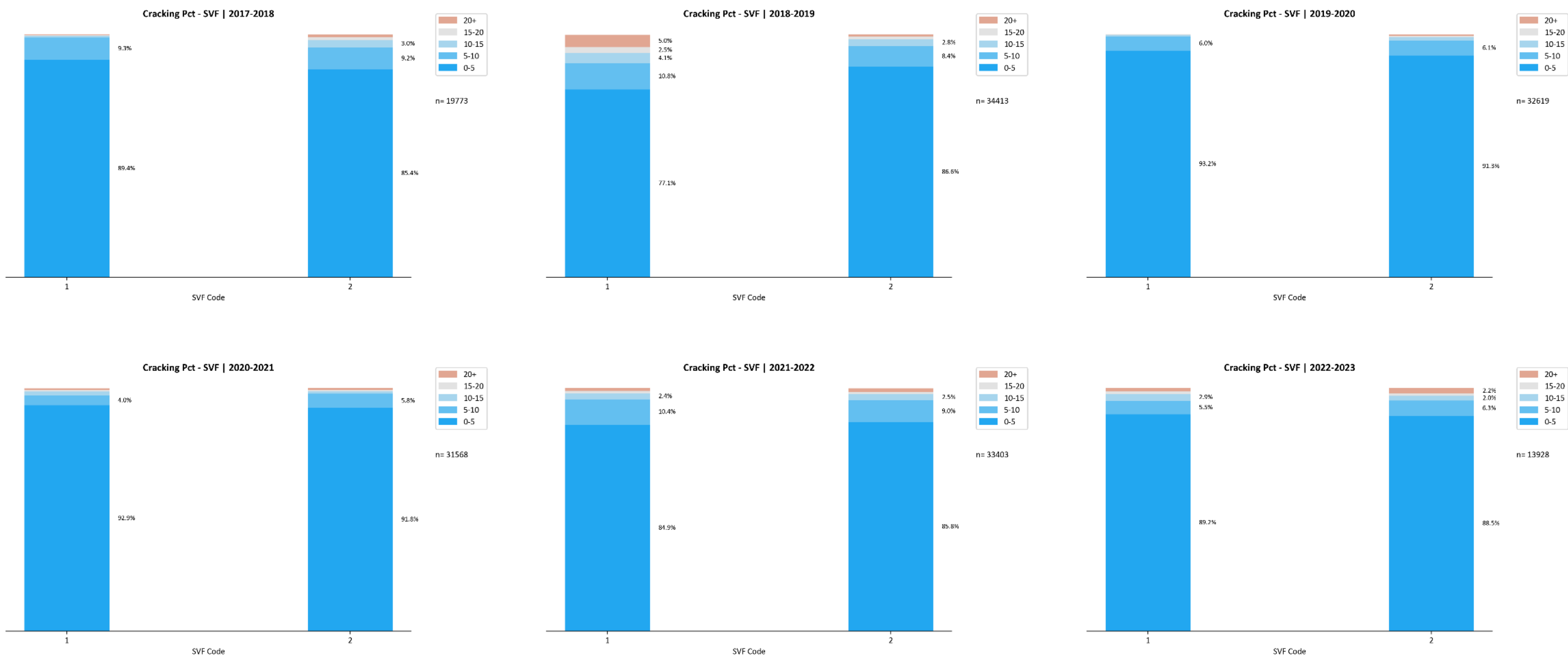

Figure 36 - Year-to-year cracking percent deterioration range distributions based on seasonal variation factor (SVF)

B.20 Cracking Percent: ESAL

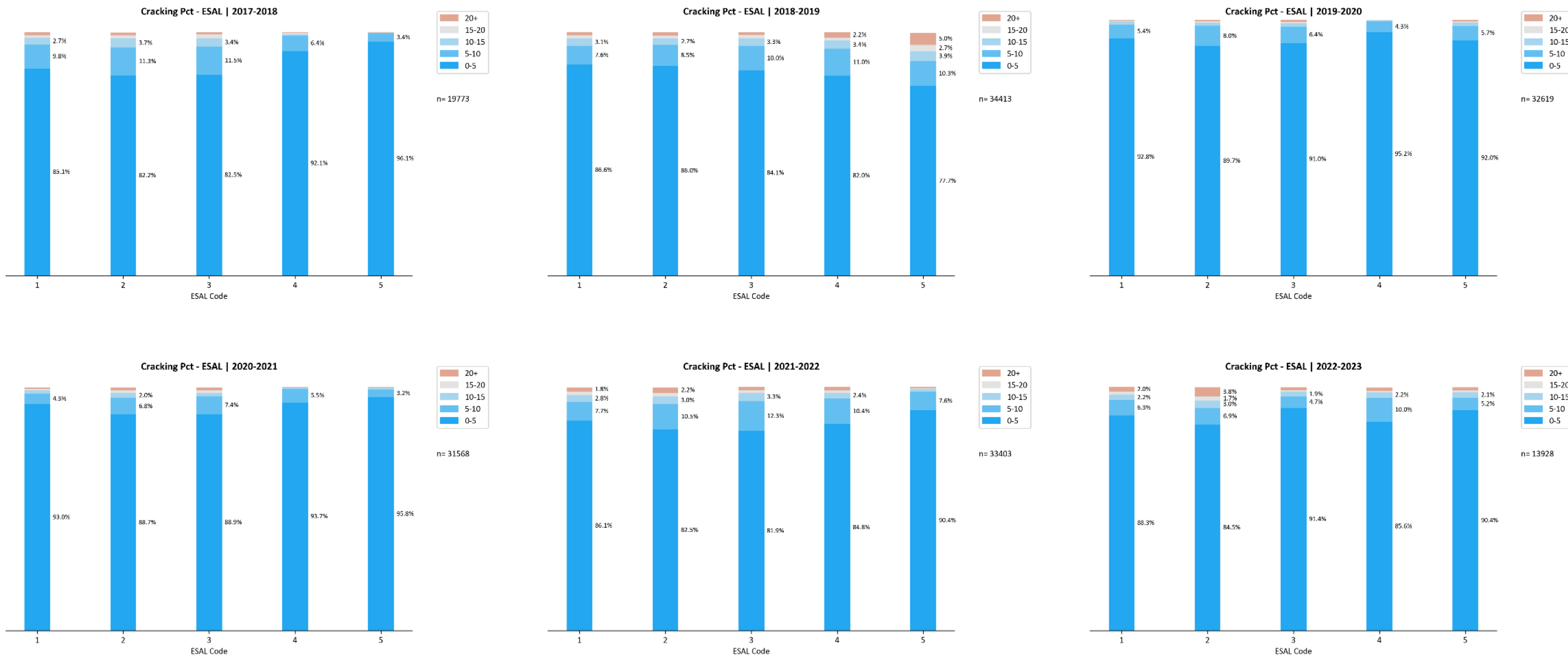

Figure 37 - Year-to-year cracking percent deterioration range distributions based on equivalent single axial load (ESAL)

B.21 Cracking Percent: Foundation

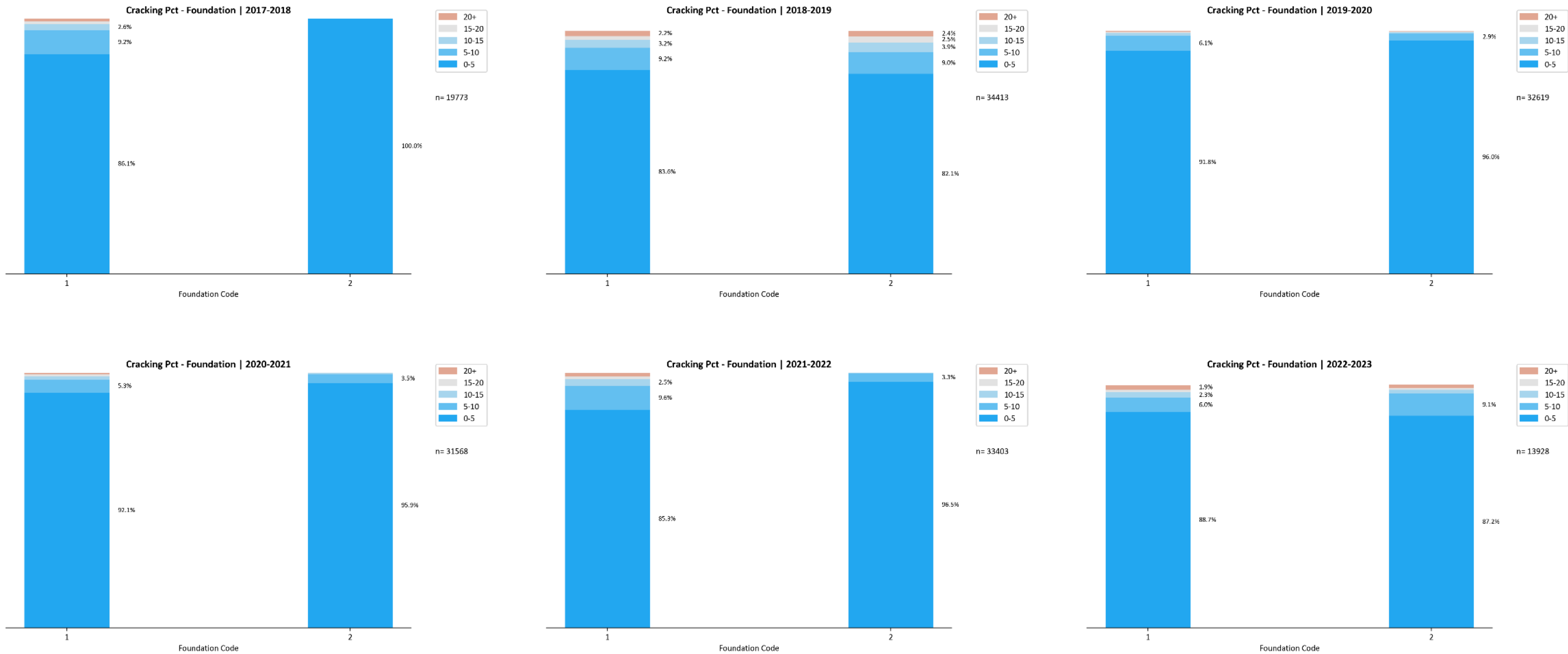

Figure 38 - Year-to-year cracking percent deterioration range distributions based on foundation issues

B.22 Max Faulting Height: Pavement Type

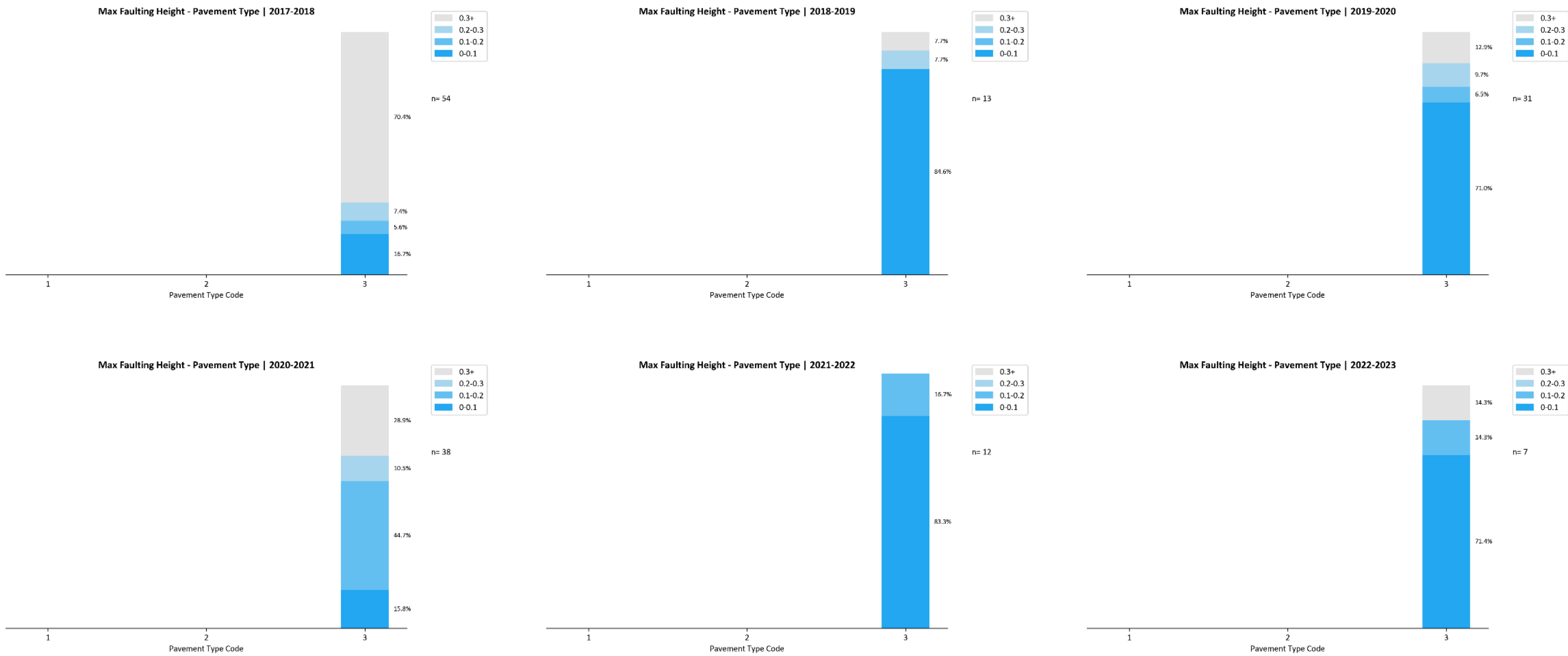

Figure 39 Year-to-year max faulting height deterioration range distributions based on pavement type

B.23 Max Faulting Height: SVF

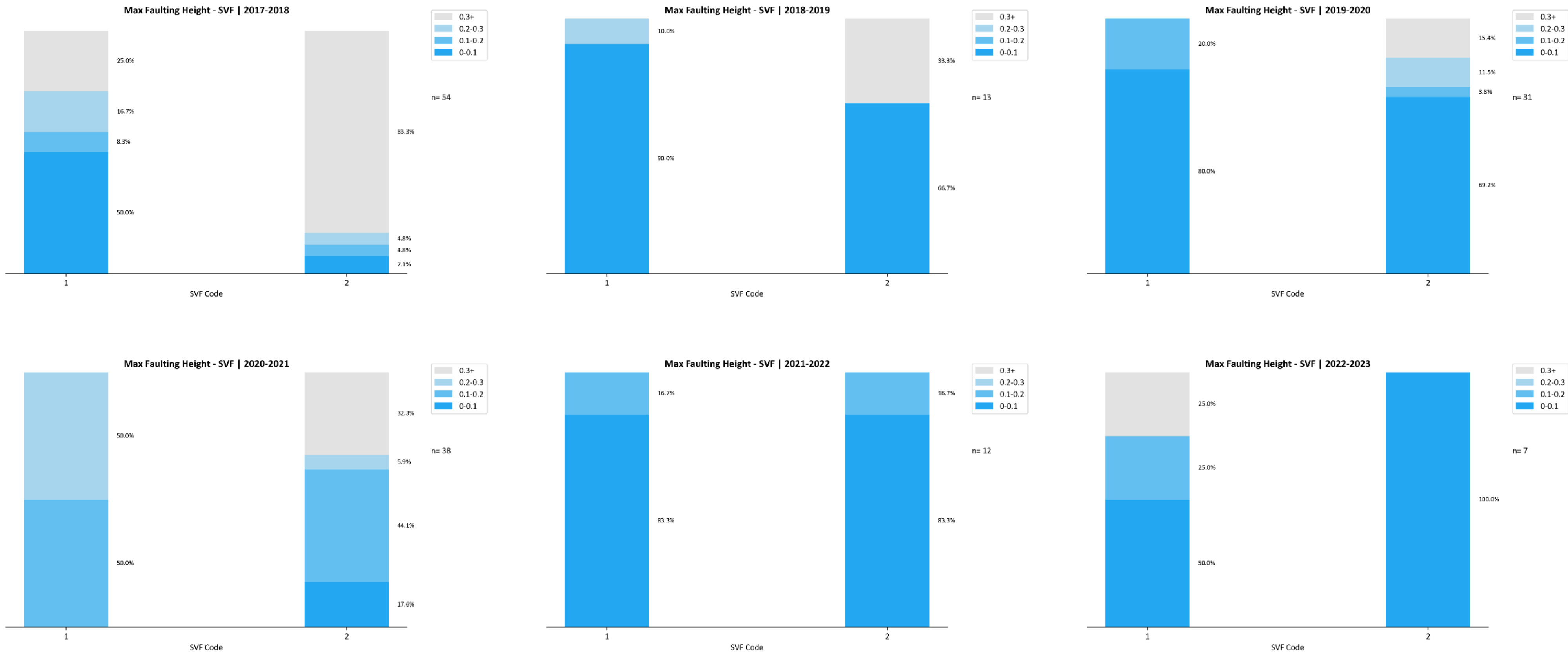

Figure 40 - Year-to-year max faulting height deterioration range distributions based on seasonal variation factor (SVF)

B.24 Max Faulting Height: ESAL

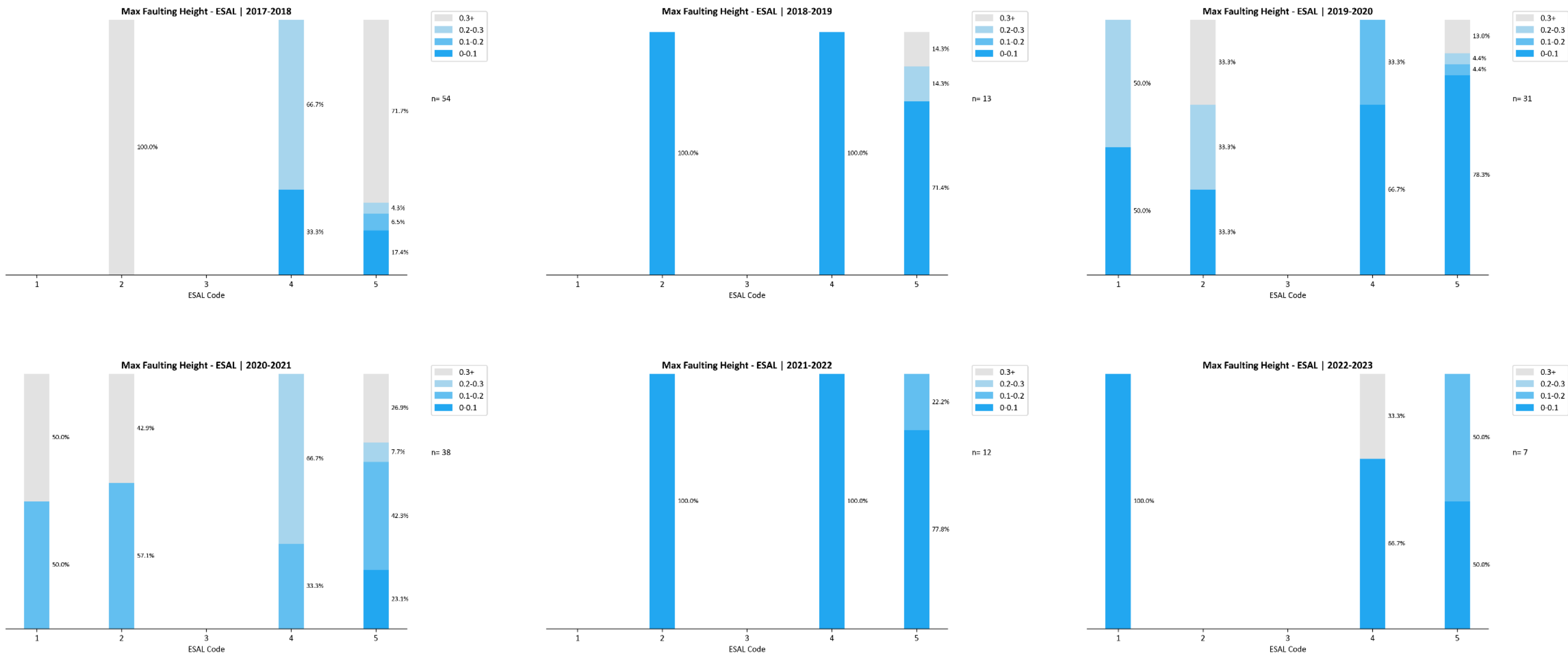

Figure 41 - Year-to-year max faulting height deterioration range distributions based on equivalent single axial load (ESAL)

B.25 Max Faulting Height: Foundation

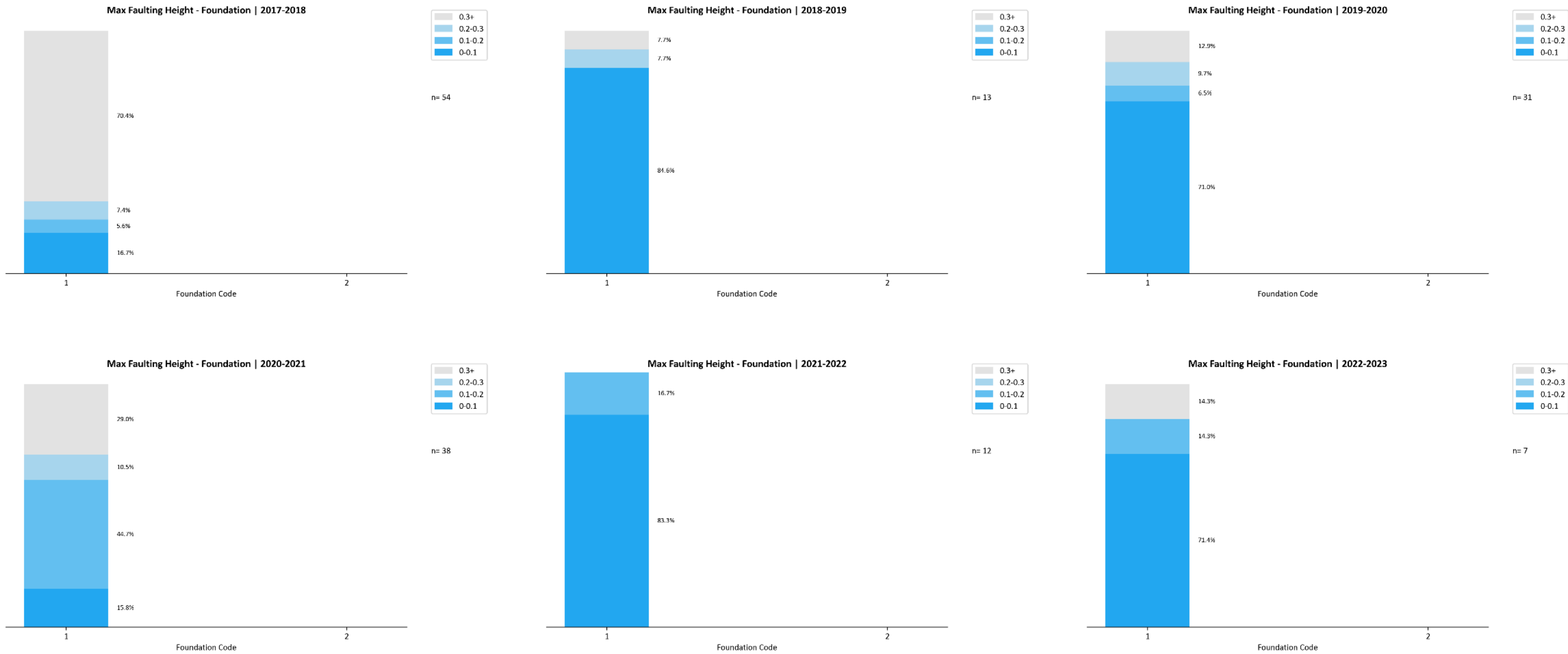

Figure 42 - Year-to-year max faulting height deterioration range distributions based on foundation issues

B.26 Mean Faulting Height: Pavement Type

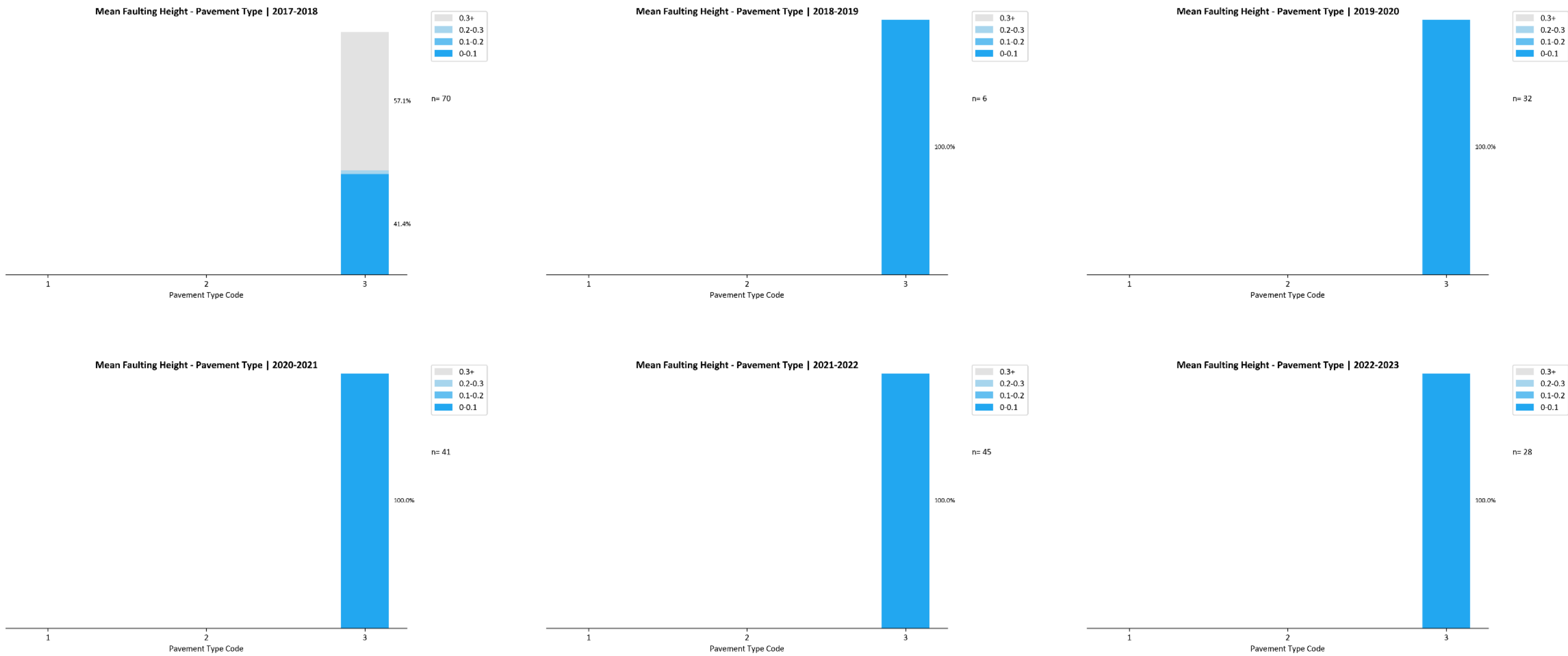

Figure 43 Year-to-year mean faulting height deterioration range distributions based on pavement type

B.27 Mean Faulting Height: SVF

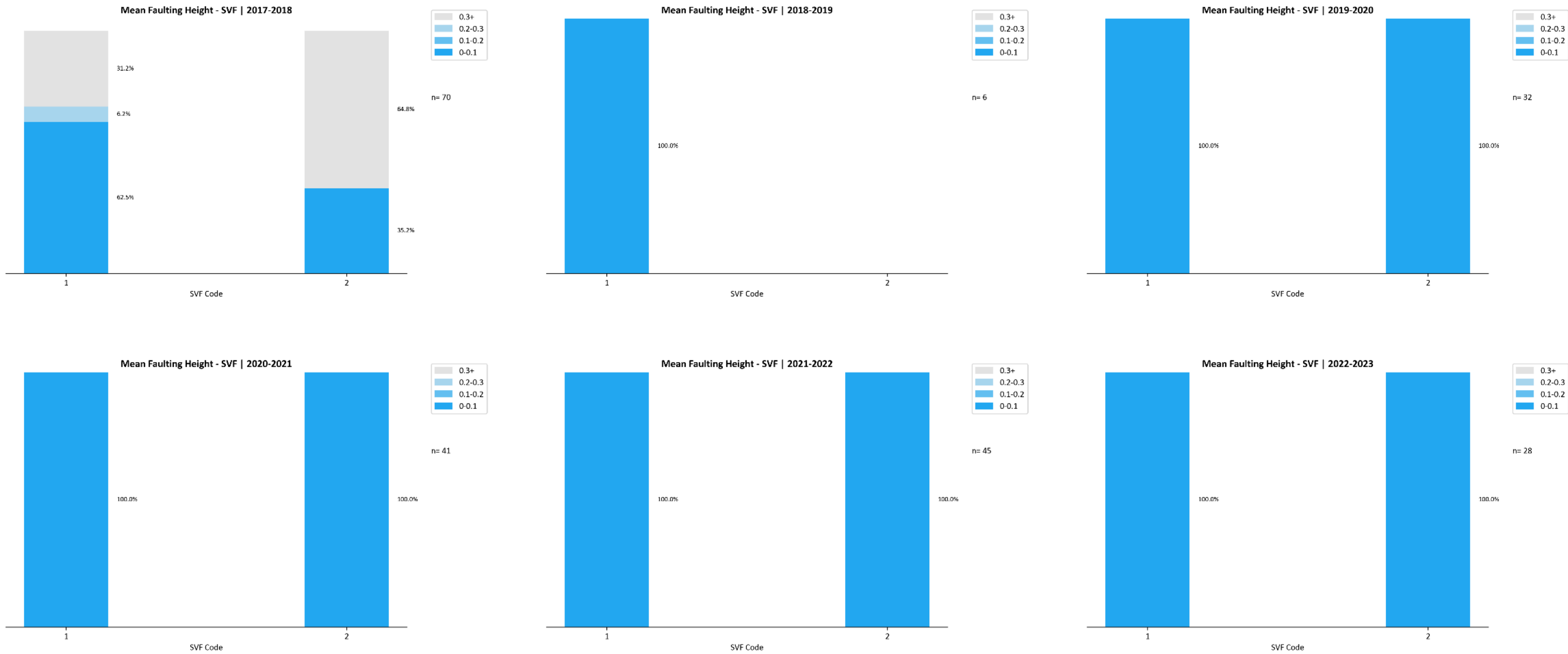

Figure 44 - Year-to-year mean faulting height deterioration range distributions based on seasonal variation factor (SVF)

B.28 Mean Faulting Height: ESAL

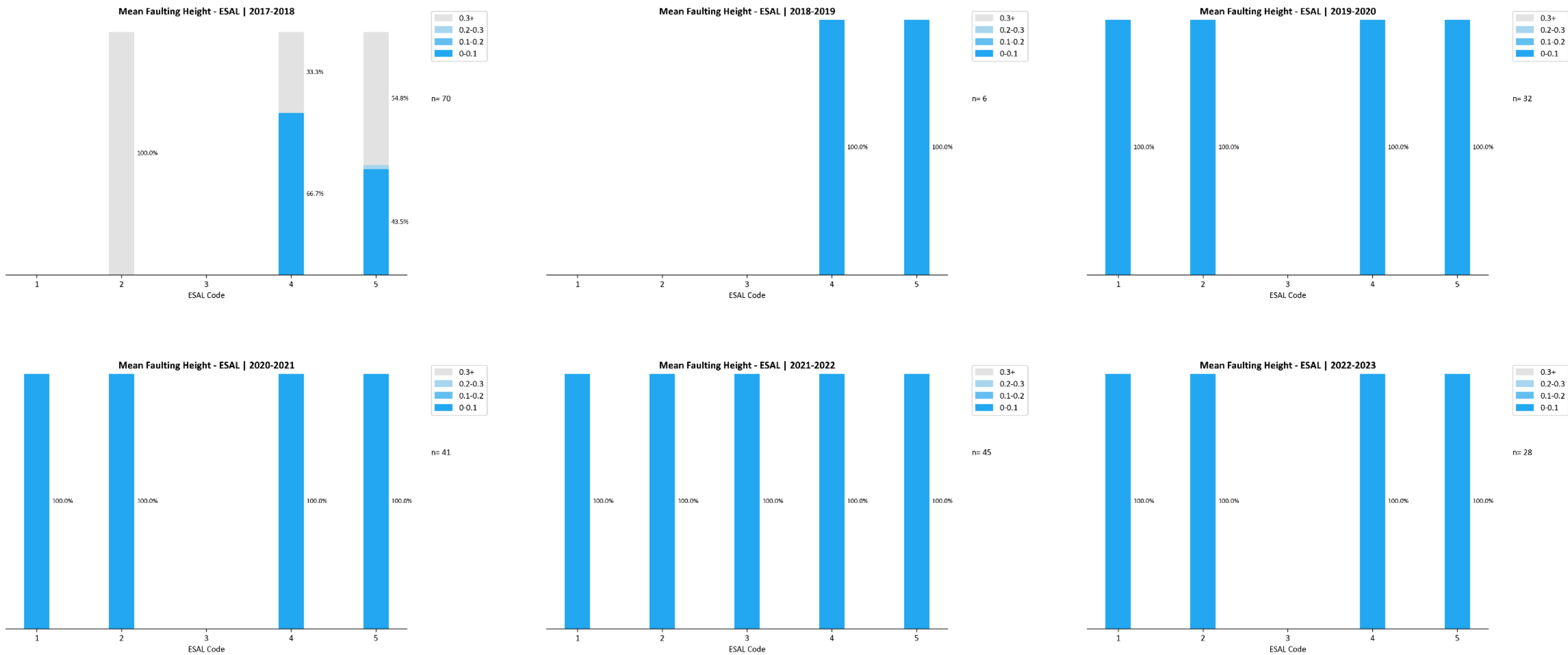

Figure 45 - Year-to-year mean faulting height deterioration range distributions based on equivalent single axial load (ESAL)

B.29 Mean Faulting Height: Foundation

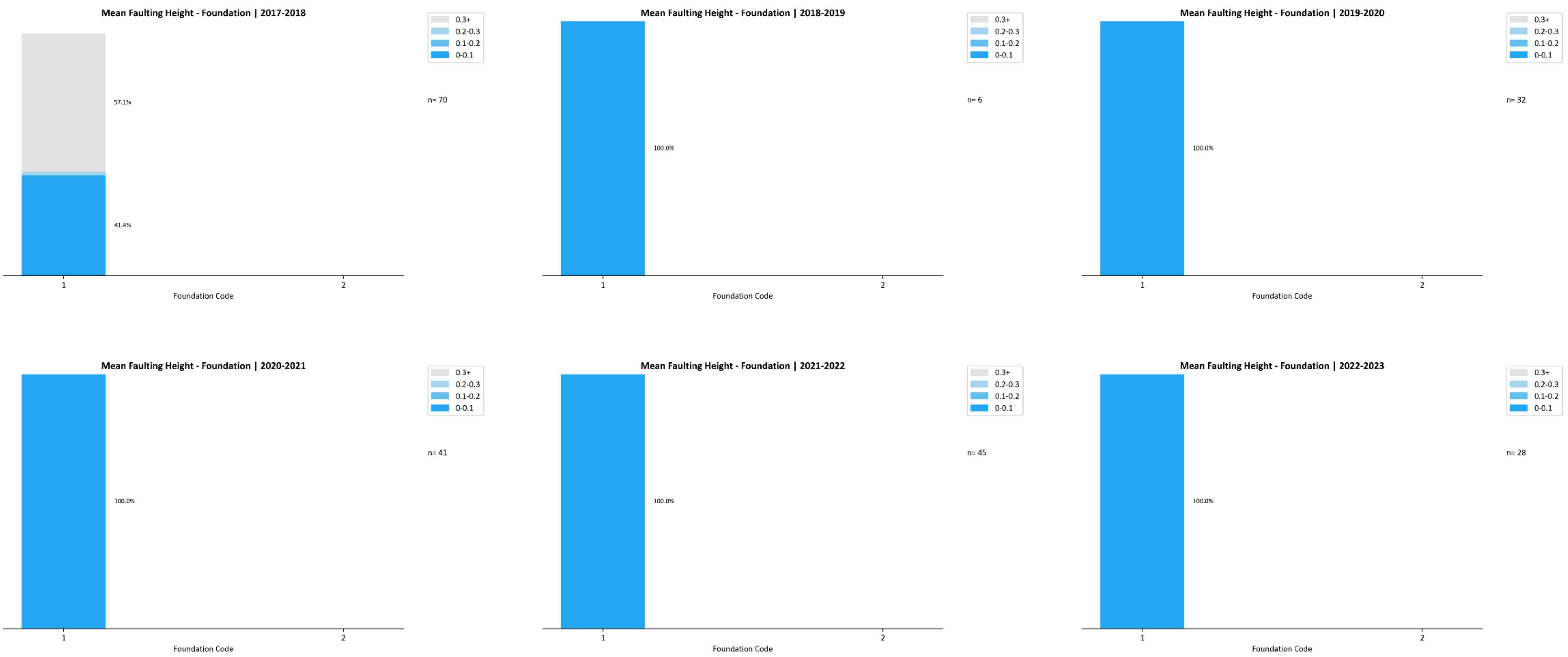

Figure 46 - Year-to-year mean faulting height deterioration range distributions based on foundation issues